Received: 10 January 2019 | Revised: 19 March 2019 | Accepted: 23 March 2019

DOI: 10.1002/hbm.24591

RESEARCH ARTICLE

WILEY

Altered static and dynamic functional network connectivity in Alzheimer's disease and subcortical ischemic vascular disease: shared and specific brain connectivity abnormalities

Zening Fu[1] | Arvind Caprihan[1] | Jiayu Chen[1] | Yuhui Du[1,2] | John C. Adair[3] | Jing Sui[1,4] | Gary A. Rosenberg[3] | Vince D. Calhoun[1,5]

[1]The Mind Research Network, Albuquerque, New Mexico

[2]School of Computer and Information Technology, Shanxi University, Taiyuan, China

[3]Department of Neurology, University of New Mexico Health Sciences Center, Albuquerque, New Mexico

[4]Chinese Academy of Sciences (CAS), Centre for Excellence in Brain Science and Intelligence Technology, University of Chinese Academy of Sciences, Beijing, China

[5]Department of Electrical and Computer Engineering, University of New Mexico, Albuquerque, New Mexico

Correspondence
Zening Fu, The Mind Research Network, 1101 Yale Boulevard NE, Albuquerque, NM 87106
Email: fzn198637@gmail.com; zfu@mrn.org

Funding information
National Institutes of Health, Grant/Award Numbers: 1UH2NS100598-01, P20GM103472, R01EB006841, R01REB020407

Abstract

Subcortical ischemic vascular disease (SIVD) is a major subtype of vascular dementia with features that overlap clinically with Alzheimer's disease (AD), confounding diagnosis. Neuroimaging is a more specific and biologically based approach for detecting brain changes and thus may help to distinguish these diseases. There is still a lack of knowledge regarding the shared and specific functional brain abnormalities, especially functional connectivity changes in relation to AD and SIVD. In this study, we investigated both static functional network connectivity (sFNC) and dynamic FNC (dFNC) between 54 intrinsic connectivity networks in 19 AD patients, 19 SIVD patients, and 38 age-matched healthy controls. The results show that both patient groups have increased sFNC between the visual and cerebellar (CB) domains but decreased sFNC between the cognitive-control and CB domains. SIVD has specifically decreased sFNC within the sensorimotor domain while AD has specifically altered sFNC between the default-mode and CB domains. In addition, SIVD has more occurrences and a longer dwell time in the weakly connected dFNC states, but with fewer occurrences and a shorter dwell time in the strongly connected dFNC states. AD has both similar and opposite changes in certain dynamic features. More importantly, the dynamic features are found to be associated with cognitive performance. Our findings highlight similar and distinct functional connectivity alterations in AD and SIVD from both static and dynamic perspectives and indicate dFNC to be a more important biomarker for dementia since its progressively altered patterns can better track cognitive impairment in AD and SIVD.

KEYWORDS

Alzheimer's disease (AD), cognitive impairment, dynamic functional network connectivity (dFNC), resting-state functional network connectivity (rs-FNC), subcortical ischemic vascular disease (SIVD)

1 | INTRODUCTION

Vascular cognitive impairment and dementia (VCID), due to disease of the small vessels, produces a progressive decline in cognition related to pathological changes in the vascular system (Hachinski et al., 2006; Zhang et al., 2013). VCID, which is the second most common type of dementia after Alzheimer's disease (AD), has aroused widespread concern because of its high occurrences in older individuals and its potential relationships to the pathogenesis of AD (Corriveau et al., 2016; Román, 2002a; Rosenberg, 2017). Subcortical ischemic vascular

disease (SIVD), a clinically homogeneous disease resulting from lacunar infarcts and hypoxic hypoperfusion of the deep white matter (WM), is a major cause of VCID (Román, Erkinjuntti, Wallin, Pantoni, & Chui, 2002b; Sun et al., 2011). The clinical features of SIVD share overlapping symptoms with AD, such as psychomotor slowness, loss of memory, and changes in speech and mood (Román et al., 2002b), making the clinical differentiation of SIVD from AD at times difficult (Jagust, 2001). It is estimated that over half of AD patients present with white-matter infarction and patients with vascular dementia may also meet the criteria for AD (Sarangi, San Pedro, & Mountz, 2000). However, there is still a lack of criteria for distinguishing these two forms of dementia, and research efforts are underway to elucidate more reliable and applicable brain abnormalities and biomarkers to improve clinical diagnosis.

Resting-state functional connectivity (rs-FC) derived from functional magnetic resonance imaging (fMRI) reflects synchronizations between spontaneous neurophysiological events in spatially remote brain regions (Biswal, Zerrin Yetkin, Haughton, & Hyde, 1995; Cordes et al., 2001; Greicius, Krasnow, Reiss, & Menon, 2003). There have been numerous research efforts using rs-FC to examine the functional organization of the brain in various psychiatric disorders, such as schizophrenia (Calhoun & Adali, 2012; Jafri, Pearlson, Stevens, & Calhoun, 2008), autism (Cerliani et al., 2015; Kana, Keller, Cherkassky, Minshew, & Just, 2006), and different types of dementia including AD (Dai et al., 2012; Greicius, Srivastava, Reiss, & Menon, 2004; Wang et al., 2006) and SIVD (Sang et al., 2018; Sun et al., 2011; Zhang et al., 2013). Specifically, reported rs-FC changes in AD in comparison to healthy controls (HCs) have mainly involved the frontal, sensorimotor (SM), parietal, default-mode (DM), and cerebellar (CB) regions (Agosta et al., 2012; Badhwar et al., 2017; Jones et al., 2011; Tucholka et al., 2018; Zheng, Liu, Song, Li, & Wang, 2017), most of which also showed abnormalities in patients with SIVD or WM hyperintensities (WMHs) (Cheng et al., 2017; Liang et al., 2016; Sun et al., 2014; Yi et al., 2012). For instance, Zheng et al. (2017) have found that patients with AD show decreased rs-FC in visual and SM networks, which are significantly associated with cognitive decline. Similarly, disrupted rs-FC associated with visual and SM networks have been identified in SIVD patients (Sun et al., 2011; Zhang et al., 2013). Previous studies also reported AD-related rs-FC abnormalities in frontal–parietal, subcortical (SC), and CB networks (Binnewijzend et al., 2012; Wang et al., 2007), which are widely observed in patients with WM diseases (Liang et al., 2016; Sang et al., 2018). However, most of the previous studies focused on just one type of dementia (e.g., AD or SIVD), ignoring the comparison and relationship between them. The exploration of shared and specific rs-FC abnormalities between different dementias can help to capture reliable biomarkers for clinical assessment and advance the knowledge of the pathological mechanism underlying AD and SIVD.

In addition, the above-mentioned research employed static rs-FC that may be limited because of the assumption of spatial and temporal stationarity of functional interactions throughout the resting-state (Allen et al., 2014; Chang & Glover, 2010). Recent progress in fMRI studies has provided a large body of evidence showing that the fluctuations in FC are of neural origin and even more prominent during the resting period when mental activity is unconstrained (Allen et al., 2014; Calhoun, Miller, Pearlson, & Adalı, 2014; Hutchison, Womelsdorf, Allen, et al., 2013a; Hutchison & Morton, 2015; Hutchison, Womelsdorf, Gati, Everling, & Menon, 2013b). Although there has been work using dynamic rs-FC to investigate impairments in AD (de Vos et al., 2018; Guo, Liu, Chen, Xu, & Jie, 2017), it is unclear whether dynamic rs-FC is similarly affected in SIVD and whether dynamic rs-FC can provide additional information about SIVD and AD beyond static rs-FC. In our previous work, we have proposed a dynamic analysis framework that is based on group independent component analysis (ICA) (Calhoun, Adali, Pearlson, & Pekar, 2001), the Pearson correlation coefficient, sliding window approach, and k-means clustering to characterize dynamic changes in whole-brain rs-FC (or its among-network relative, functional network connectivity [FNC], which focuses on connectivity between networks) associated with brain disorders (Damaraju et al., 2014; Fu et al., 2017; Fu et al., 2018). This framework has been widely employed in neuroscience research and has successfully identified numerous dynamic FNC (dFNC) biomarkers for different brain disorders, including schizophrenia (Damaraju et al., 2014; Du et al., 2018; Fu et al., 2017), bipolar disorder (Rashid et al., 2016; Rashid, Damaraju, Pearlson, & Calhoun, 2014), autism (Fu et al., 2018), and Parkinson's disease (Kim et al., 2017). For example, Kim et al. applied this framework to study Parkinson's disease, showing that they have fewer occurrences in the sparsely connected dynamic state but more in the strongly interconnected dynamic state. Interestingly, the opposite findings are observed in schizophrenia, where patients with schizophrenia spend more time in a disconnected state (Damaraju et al., 2014; Du, Pearlson, et al., 2016b).

Herein, to fully and systematically explore the rs-FC abnormalities that are associated with different types of dementia, we combined a dFNC analysis framework with a static FNC (sFNC) analysis and studied the brain connectivity changes from both static and dynamic perspectives. To our knowledge, no prior work has investigated static and dFNC changes in SIVD and AD individuals and compared such changes between them. Traditional group ICA studies generally estimated group-level independent components (ICs) using only the discovery data set and therefore the identified target components are variable across studies (Allen et al., 2014; Calhoun et al., 2001; Miller, Yaesoubi, & Calhoun, 2014). In the present study, we performed group ICA on two independent public available data sets with large sample sizes and matched their estimated group components for further intrinsic connectivity networks (ICNs) identification to overcome this limitation. With the help of a spatially constrained ICA approach (Du, Allen, et al., 2016a; Du & Fan, 2013), we estimated subject-specific component spatial maps and time courses for our VCID data sets. The homologous and heterogeneous symptoms between SIVD and AD led us to hypothesize the presence of both similar and distinct changes in sFNC and dFNC between these two patient groups. We also hypothesized that the altered FNC features would be associated with the levels of cognitive impairment and the dFNC might provide more information on cognitive impairments that cannot be captured from the sFNC.

2 | METHODS

2.1 | Participants

The data set was from an ongoing study of VCID at the University of New Mexico (UNM). All participants provided written informed consent approved by the UNM Human Research Protections Office. This data set included 159 subjects who received resting-state fMRI scans. All subjects underwent a research level MRI and a cerebrospinal fluid biochemical analysis (Erhardt et al., 2018; Jack et al., 2018; Rosenberg et al., 2016). HCs were recruited from the community with normal neuropsychological and neurological examinations. Patients were recruited from the neurologists' cognitive disorders clinics. Three neurologists arrived at a consensus diagnosis after reviewing the medical history, physical and neurological examinations, clinical MRI, and basic laboratory studies for the diagnosis of patients. The patients comprised a diverse group diagnosed with different causes of cognitive dysfunction (e.g., Parkinson's disease, dementia with Lewy bodies, frontotemporal dementia, psychiatric disorders, AD, and SIVD).

In the present study, we selected data samples according to the following criteria: (a) patients diagnosed with AD based on McKhann criteria for probable diagnosis (McKhann et al., 1984); (b) patients diagnosed with SIVD show extensive SC WM signal abnormality with clinical support for ischemic injury (gait disorder, focal exam abnormality); (c) HCs without any dementia diagnosis history; (d) subjects with head motion ≤3° and ≤3 mm; and (e) subjects with functional data providing near full brain successful normalization (by comparing the individual mask with the group mask. Detailed procedures are provided in Appendix S1). These criteria yielded a total of 76 subjects (38 HCs, 19 patients with AD, and 19 patients with SIVD) in which the controls and patients were matched by number and age (p = 0.1843, analysis of variance [ANOVA]). Among the selected subjects, 74 subjects had been assessed with cognitive tests. Cognitive tests were administered by a trained research psychologist (JP) and trained research coordinators and scored according to standard procedures. Standardized (T) scores were calculated for each test. Average composite T-scores were calculated for five domains: memory (Hopkins Verbal Learning Test-Delay, Rey Complex Figure Test-Long Delay), executive function (Digit Span Backwards, Trail Making Test B, Stroop Interference Score, and Controlled Oral Word Association [FAS]), attention (Digit Span Forward, and Trial Making Test A), language (Boston Naming 60 item test, Controlled Oral Word Association [Animals]), and processing speed (Digit Symbol and Symbol Search, both based on WAIS-3). HCs underwent the same neuropsychological test battery. Demographic information is provided in Table 1. Past research has demonstrated multiple tests can provide a more reliable estimate of a cognitive construct than any single test (Anastasi & Urbina, 1997). It is also suggested that the objective tests should focus on multiple cognitive domains to increase the ability to detect full cognitive impairments (Bondi et al., 2014; Ferman et al., 2013; Loewenstein et al., 2009). Our study performed a comprehensive neuropsychological assessment for each participant and the test scores were assigned to different cognitive domains. We believed that the use of summarized scores for different cognitive domains would help capture more reliable cognitive impairments in dementia.

2.2 | Data sets acquisition and preprocessing

All participants were scanned during a rest condition with eyes closed. The study's fMRI scans were acquired on a 3T Siemens TIM Trio scanner. This ongoing VCID study employed two different head coils, a 12-channel radio-frequency (RF) coil and a 32-channel RF coil with a multiband sequence during different stages of recruitment. The 12-channel fMRI data were scanned using gradient-echo echo planar imaging (EPI) with a field of view (FOV) = 240 mm; a 3.5 mm slice thickness, and 30% distance factor; a 3.75×3.75 mm^2 in-plane resolution, repetition time (TR) = 2000 ms, echo time (TE) = 29 ms; anterior–posterior (AP) phase encoding direction; and 165 measurements collected for a total acquisition time of 5.5 min. The 32-channel fMRI data were acquired using a multiband EPI sequence with an FOV = 248 mm; $3 \times 3 \times 3$ mm^3 voxel resolution; multiband factor = 8, TR = 460 ms, TE = 29 ms; AP phase encoding direction; and 650 measurements collected for a total acquisition time of 5 min. Data for distortion correction were collected using two additional EPI spin-echo sequences run in AP and posterior–anterior (PA) phase encoding directions. The image resolution, echo-spacing, and bandwidth of the EPI fMRI sequence and the EPI spin-echo sequence were matched.

The fMRI data were preprocessed using a combination of toolboxes: AFNI3 (https://afni.nimh.nih.gov), SPM12 (http://www.fil.ion.ucl.ac.uk/spm/), GIFT4.0b (http://mialab.mrn.org/software/gift), and custom code written in MATLAB. A slice-timing correction was first performed to account for timing differences in slice acquisition. After that, a rigid body motion correction was performed to correct the head motion of the fMRI scans. A despiking procedure was then conducted on the fMRI data using the AFNI3 3dDespike algorithm to mitigate the impact of outliers. The fMRI data were subsequently warped to a Montreal Neurological Institute space using the tissue probabilistic maps in the SPM toolbox and were resampled to 3 mm^3 isotropic voxels. Finally, the fMRI data were smoothed using a full width at half maximum Gaussian kernel of 6 mm. We performed additional distortion correction on the 32-channel fMRI data. Before motion correction, a distortion field was calculated from the AP and PA phase-encoded EPI data by the TOPUP/FSL algorithm (Andersson, Skare, & Ashburner, 2003) and used to correct the fMRI scans.

2.3 | Framework for static and dynamic connectivity in AD and SIVD

The framework used to investigate AD and SIVD for specific and common connectivity changes and their associations with cognitive performance is as follows (shown in Figure 1): (a) group ICA was performed and individual spatial maps and time courses were computed using spatially constrained ICA with the group template as a prior; (b) sFNC was calculated using the Pearson correlation coefficient and group differences were examined; (c) dFNC was calculated using a

TABLE 1 Participant demographics

Phenotypic	HC, mean (*SD*)	AD, mean (*SD*)	SIVD, mean (*SD*)	*p*-Value (ANOVA)
Age (76 subjects)	65.82 (10.15)	70.47 (8.46)	68.05 (6.80)	0.1843
Executive (74 subjects)	50.11 (6.00)	42.89 (8.17)	40.16 (8.71)	.0033
Memory (74 subjects)	54.38 (10.98)	30.61 (8.59)	45.32 (11.32)	6.52e-8
Attention (74 subjects)	52.81 (7.11)	46.11 (11.17)	40.47 (9.83)	.0021
Language (74 subjects)	54.30 (8.30)	42.94 (11.30)	44.42 (10.36)	.0034
Processing speed (74 subjects)	56.24 (7.25)	47.83 (12.00)	43.84 (8.41)	.0022

Abbreviations: AD, Alzheimer's disease; ANOVA, analysis of variance; HC, healthy control; SIVD, subcortical ischemic vascular disease.

sliding window approach and a k-means clustering-based state analysis were conducted on dFNC estimates. The group difference in fraction rate of occurrences and mean dwell time of dFNC states was examined; and (d) altered static and dynamic features (sFNC, occurrences and mean dwell time of dFNC states) were correlated with cognitive scores to investigate potential associations between neuroimaging features and cognitive impairment.

2.4 | Group ICA

Previous studies typically conducted group ICA on the exploratory data set and identified targeted ICs as ICNs for FNC analysis. However, due to the difference among data sets (e.g., sample size, data dimensions, or data qualities), the identified ICNs are variable and not necessarily consistent across studies. Therefore, to identify reliable ICNs that are robust and consistent across data sets, we performed group ICA on two independent data sets with large sample sizes and different temporal resolutions (Human Connectome Project and Genomics Superstruct Project [GSP], details are provided in Appendix S1).

ICs from the two data sets were matched by comparing their corresponding group-level spatial maps. We examined whether an IC from one data set has a matched IC from the other data set when their spatial correlation is larger than 0.25. A correlation value around 0.25 is a reasonable choice for showing the correspondence between ICs from different data sets (Segall et al., 2012; Smith et al., 2009). This threshold also conservatively represents a significance level of $p < .005$, corrected (Smith et al., 2009). Then, we characterized a subset of matched ICs as ICNs by considering their peak activations and power spectrum. ICNs should exhibit peak activations in gray matter; have low spatial overlap with known vascular, ventricular, motion, and susceptibility artifacts; and have dominant low-frequency fluctuations on their time courses (Allen et al., 2014). ICNs were categorized into different domains based on anatomy and prior knowledge of their function (Allen et al., 2014; Allen, Damaraju, Eichele, Wu, & Calhoun, 2018; Damaraju et al., 2014). The components were evaluated by three experts. After identifying the ICNs, we used the group template of GSP data set as a reference within a spatially constrained ICA algorithm to compute individual spatial maps and time-courses for the VCID data set (Du et al., 2016a). Before calculating the sFNC and dFNC between time courses of ICNs, we conducted post-processing procedures on time courses to remove remaining noise sources, including (a) detrending linear, quadratic, and cubic trends; (b) conducting multiple regressions of the six realignment parameters and their temporal derivatives; (c) despiking detected outliers; and (d) low-pass filtering with a cutoff frequency of 0.15 Hz.

2.5 | sFNC and dFNC analysis

We calculated sFNC using the Pearson correlation coefficients between the time courses of ICNs. This resulted in an sFNC matrix with the dimension of $C \times C$ (C is the number of ICNs identified) for each subject. Since the VCID data set was scanned using two different head coils, before investigating the group differentiating sFNC, we regressed out head coil effects from each sFNC cell. Only the HCs were used for the estimation to avoid introducing confounding effects related to diseases. Diagnosis effects on sFNC were estimated in an ANOVA model, controlling age, and gender. If the effects were significant, a general linear model (GLM) including age and gender was conducted to examine the group difference between pairs of groups (HC vs. AD, HC vs. SIVD, and AD vs. SIVD).

For each subject sub = 1 … N, we estimated dFNC using a sliding window approach. Since the subject data were scanned with different head coils and thus have different temporal resolutions (TR = 0.46 and 2 s), we interpolated the subject time courses with larger TR to construct new time courses and used the same length of data for each subject. This procedure helps to control the potential impacts on the dynamic analysis caused by the different temporal resolutions. Prior studies have shown that such an interpolation strategy is valid for characterizing dynamic brain connectivity in data sets with different temporal resolutions (de Lacy, Doherty, King, Rachakonda, & Calhoun, 2017; Du et al., 2017). We used individual time courses with 630 observations for the dFNC estimation. A tapered window was obtained by convolving a rectangle (window size = 20, TRs = 9.2 s) with a Gaussian ($\sigma = 3$) to localize the data set at each time point. This window was slid in steps of 1 TR, resulting in total $T = 610$ windows. In order to capture more transient variations on the dFNC, we selected a shorter window size for the dFNC estimation. Our previous work demonstrated that the window size problem is not trivial since it stems from the fundamental bias–variance tradeoff problem in the estimation theory. Many dynamic connectivity studies chose a window size in the range of 30 s–1 min because their data sets typically have the TR = 2 s (15–30 time points are used for the estimation) and they want to

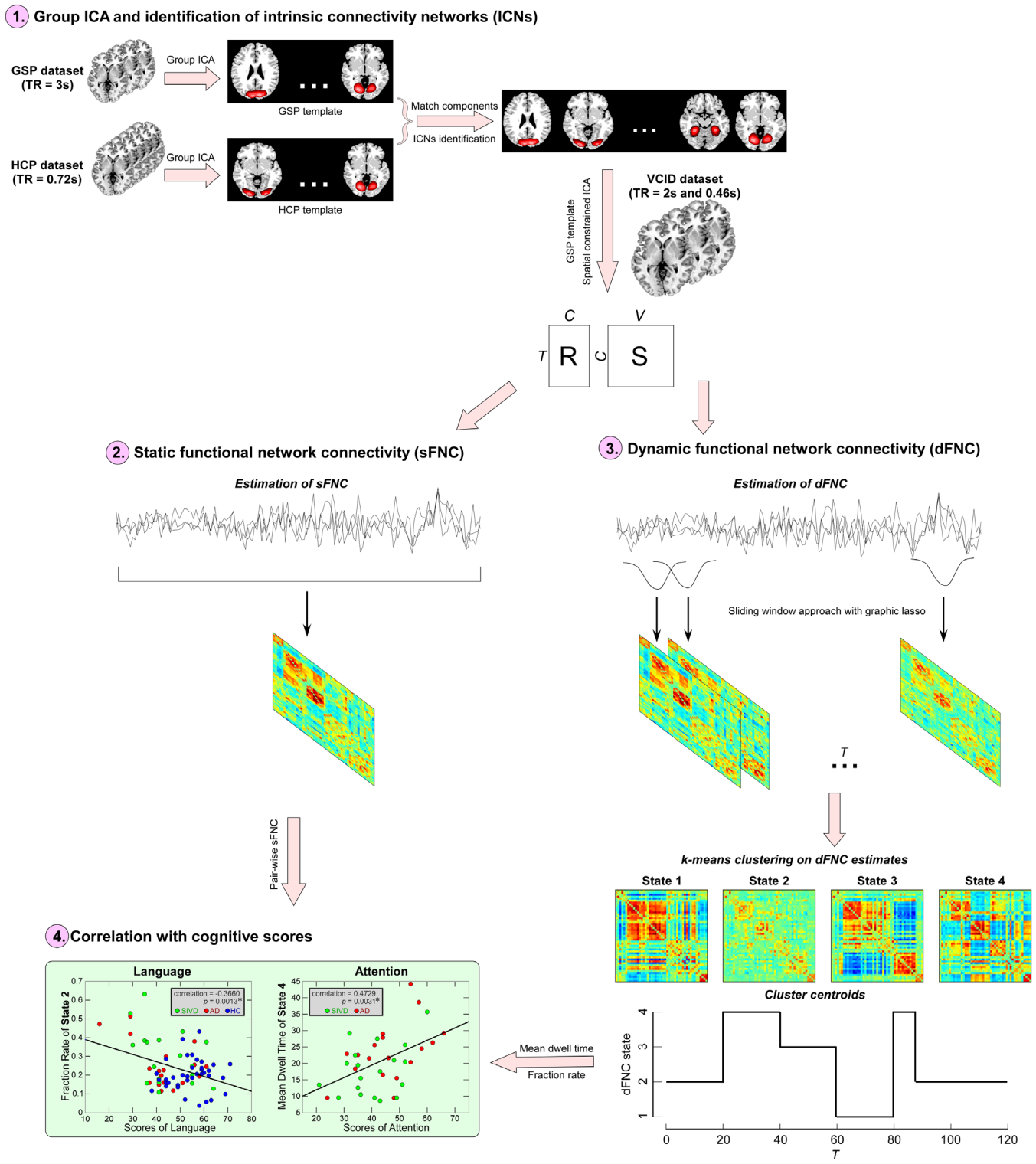

FIGURE 1 Framework of exploring altered static and dynamic functional network connectivity (FNC) in subcortical ischemic vascular disease (SIVD) and Alzheimer's disease (AD). Step 1: perform group independent component analysis (ICA) on two independent data sets and compute individual spatial maps and time courses using spatially constrained ICA with spatial priors from the exploratory data set; Step 2: estimate static FNC (sFNC) using the Pearson correlation coefficient; Step 3: estimate dynamic FNC (dFNC) using a sliding window approach and perform a k-means clustering on dFNC estimates; and Step 4: conduct correlation analysis between cognitive scores and sFNC/dFNC features [Color figure can be viewed at wileyonlinelibrary.com]

achieve a balance between estimation accuracy and capturing the transient patterns. With the multiband sequence technique, our VCID data set has a relatively shorter TR. Such a high temporal resolution helps to improve the dFNC estimation in a shorter window (20 time points are available within each window, which is comparable with that used in most of the previous studies). Therefore, it

was reasonable to use a shorter window size in the present study for capturing more transient patterns in dFNC. We also conducted an analysis based on the dFNC estimates from other window sizes. The results were highly consistent among a wide range of window sizes (16–24 TRs), suggesting that the identified altered dFNC is not caused by random artifacts. The results of other window sizes are provided in the Appendix S1.

We calculated the covariance matrices $\sum_{sub}(t)$, $t = 1 \ldots T$, using the windowed data as estimates of dFNC between ICNs. To assess a more accurate covariance matrix, we employed a graphical LASSO method (Friedman, Hastie, & Tibshirani, 2008) to estimate the regularized inverse covariance matrix $\sum_{sub}^{-1}(t)$ and then estimated the covariance matrix $\sum_{sub}^{L1}(t)$ from the inverse covariance matrix. The regularization parameter λ was optimized for each subject by using a cross-validation framework. For each subject, the covariance matrices of windows were concatenated to form a $C \times C \times T$ array that represents the dynamic changes in brain connectivity as functions of time. Similar to the sFNC, we regressed out the head coil effect from each dFNC. We calculated the mean dFNC across time for each subject, applied the GLM to estimate the effect of head coils on mean dFNC and regressed out this effect from each windowed dFNC estimate.

After controlling the effect of head coils on the dFNC, we performed a k-means clustering state analysis on dFNC estimates to explore dFNC patterns that reoccur in time and across subjects. The basic assumption of this analysis is that during the resting-state, the whole brain functional network is not stationary, but rather switches among different dynamic states represented by distinct dFNC patterns that can in part diverge strongly from static connectivity patterns. We used the L1 norm as the distance function and clustered the windowed covariance matrices into a set of separate clusters using the k-means clustering method. The optimal number of clusters

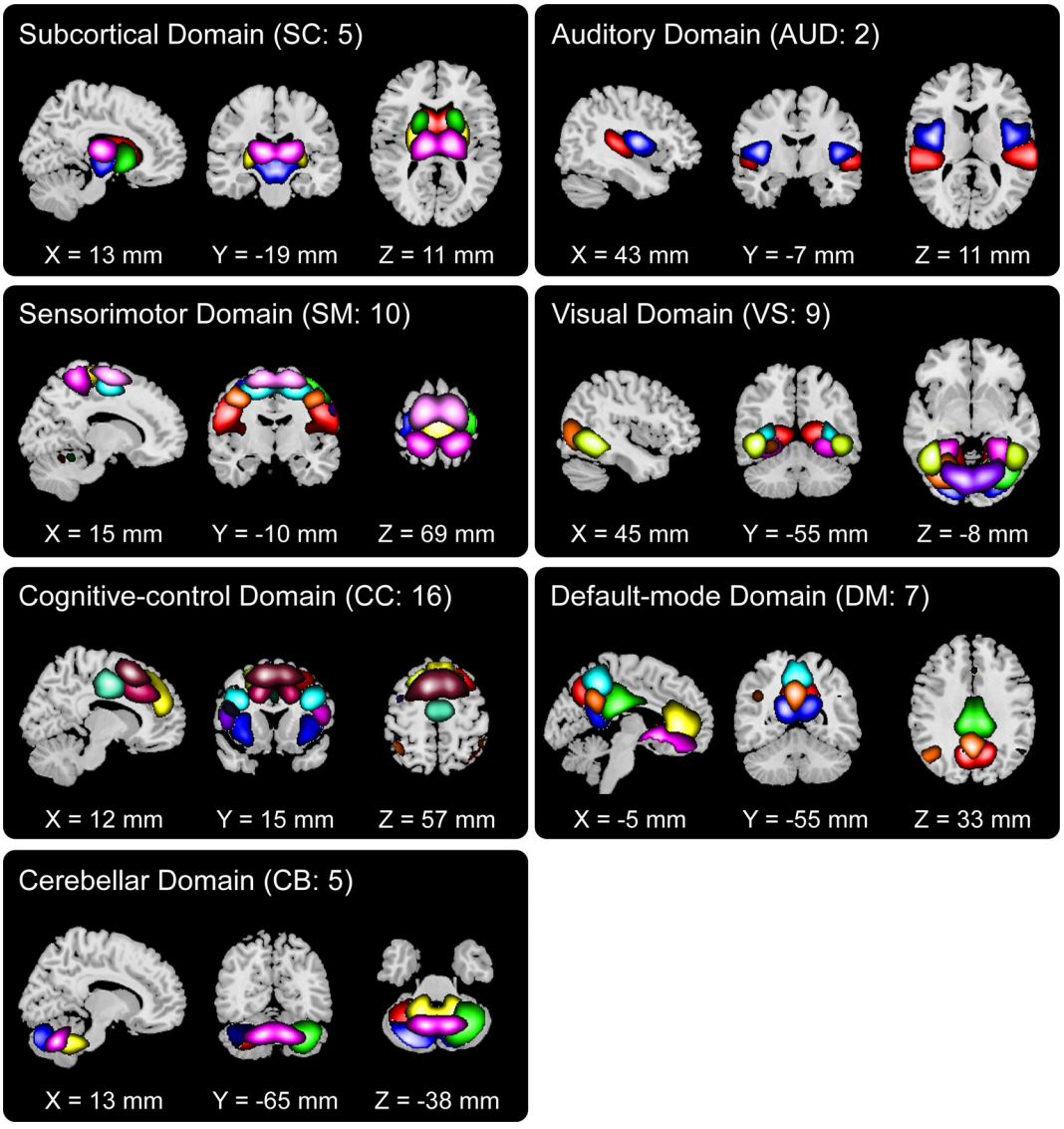

FIGURE 2 Spatial maps of identified intrinsic connectivity networks (ICNs) are divided into seven different functional domains and arranged based on their anatomical and functional properties. Each color in the composite maps corresponds to a different ICN. The detailed component labels and peak coordinates are provided in Table S1 (see supplementary materials) [Color figure can be viewed at wileyonlinelibrary.com]

was estimated by the elbow criterion, which is defined as the ratio of within clustering distance to between clusters distance. The number of clusters was determined as $k = 4$, which was within a reasonable range (4–7) consistent with our previous dFNC study on different brain disorders. We also used Akaike information criterion and Bayesian information criterion (Li, Adalı, & Calhoun, 2007) to estimate the optimal number of cluster and the results are consistent ($k = 4$). After obtaining the state vector for each subject (a vector representing which state each time point is assigned to), we divided the number of total windows (610 for every subject) by the number of windows assigned to each state to measure the fraction rate and averaged the duration window lengths of each state to measure the mean dwell time. To investigate the effect of diagnosis on the fraction rate and the mean dwell time of dynamic states, ANOVA was performed on the dynamic features controlling for age and gender. If ANOVA identified significant diagnosis effects, a GLM including age and gender was conducted to examine the group difference between pairs of groups.

2.6 | Correlation between FNC features and cognitive scores

We further examined whether sFNC and dFNC changes can predict cognitive impairment, measured using five cognitive subdomain scores. This analysis focused on those sFNC and dFNC features with significant group differences. The GLM was employed to examine the partial correlations between the cognitive scores and the abnormal imaging features in the patient groups and in the whole sample respectively, controlling for age and gender. To further prevent the potential confounding effect of group label, we repeated this analysis again by including age, gender, and diagnosis as covariates in the GLM model. All statistical results were corrected for multiple comparisons

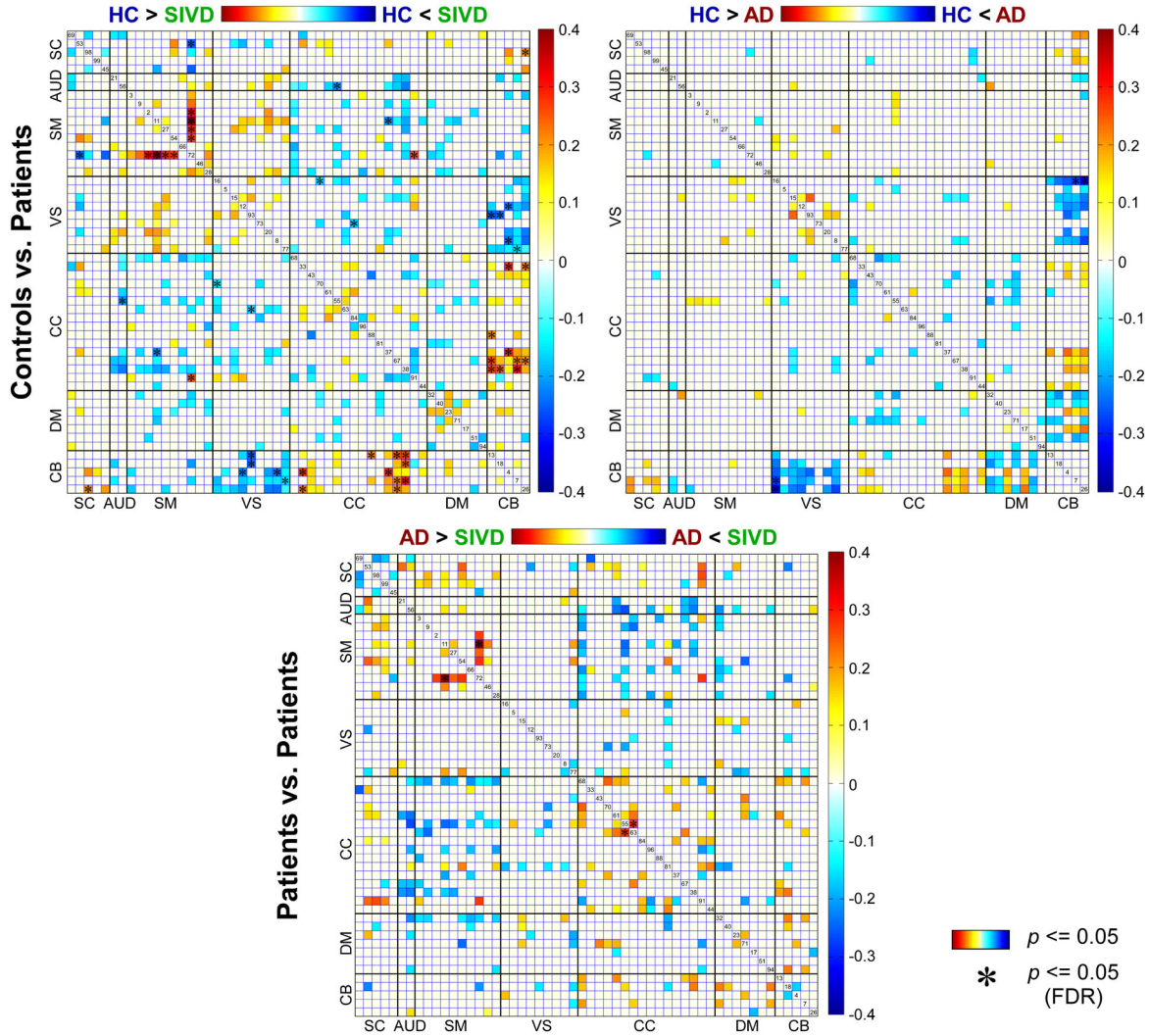

FIGURE 3 Group-discriminating static functional network connectivity (sFNC). Top left: Comparisons between healthy controls (HCs) and patients with subcortical ischemic vascular disease (SIVD); top right: Comparisons between HCs and patients with Alzheimer's disease (AD); bottom: Comparisons between SIVD and AD. sFNC with group difference ($p \leq .05$) are highlighted in red and blue. Significant group difference that passes the multiple comparisons is marked by asterisks (false discovery rate [FDR] corrected, $q = 0.05$) [Color figure can be viewed at wileyonlinelibrary.com]

using the false discovery rate (FDR) (Benjamini & Hochberg, 1995) with a correction threshold of $q = 0.05$.

3 | RESULTS

3.1 | Group ICA and ICNs identification

Figure 2 displays the spatial maps of ICNs identified with group ICA. Overall, there were 70 pairs of ICs are matched with a spatial correlation higher than 0.25, of which 54 ICs were identified as ICNs. The replicated ICNs cover the majority of SC and cortical gray matter, which are highly consistent with the results in previous high model order ICA studies. Based on the anatomical and presumed functional properties, ICNs were arranged into seven functional domains: SC domain, auditory domain, visual domain (VS), SM domain, cognitive-control (CC) domain, DM domain, and cerebellar (CB) domain. Previous studies have shown that such manual arrangement of ICNs is very similar to various orderings provided by empirical methods (Allen et al., 2014).

3.2 | Group-discriminating sFNC

The results of altered sFNC in SIVD and AD are shown in Figure 3. The comparisons were conducted between each pair of the groups (HC vs. SIVD, HC vs. AD, and SIVD vs. AD) and the results demonstrate shared and specific sFNC alterations associated with SIVD and AD. Compared with HC, SIVD has abnormal sFNC related to SM. As displayed in Figure 4, postcentral gyrus (PoCG) is a key region whose sFNCs are largely influenced in patients with SIVD. This region has atypical sFNC with multiple functional domains, such as SM (paracentral lobule [ParaCL], precentral gyrus [PreCG], and superior parietal lobule [SPL]), SC (subthalamus/hypothalamus), and CC (supplementary motor area). Most of these sFNCs significantly decrease in SIVD, except for the sFNC between PoCG and thalamus/hypothalamus, which significantly increases instead. Patients with SIVD also have increased sFNC between CB and VS, but decreased sFNC between CB and CC. According to Figure 5, the negative sFNC between the cerebellum and several visual regions, such as right middle occipital gyrus, lingual gyrus, and fusiform gyrus, change to positive correlations in SIVD. In contrast, Figure 6 shows that HCs have positive sFNC between cerebellum and CC, including middle frontal gyrus (MiFG), inferior frontal gyrus (IFG), and insula, and these sFNCs significantly decrease to negative in SIVD.

AD patients also show similar alterations in sFNC between CB and VS, and in sFNC between CB and CC, but changes are relatively weaker than that in SIVD. Figure 7 demonstrates that compared with HC, the sFNC between calcarine gyrus and cerebellum significantly increases in AD. Atypical sFNC are also observed between DM and CB, but these abnormalities are borderline significant (raw $p \leq .05$), which cannot survive in multiple comparisons. Significant group-discriminating sFNC are also observed between SIVD and AD. As shown in Figure 8, SIVD has smaller sFNC within SM (between PoCG and PreCG) and within CC (between MiFG and inferior parietal lobule [IPL]) than does AD.

3.3 | Group-discriminating dFNC features

The centroids and the count of subjects of dFNC states are displayed in the bottom row of Figures 9 and 10. Different from previous studies using larger window sizes (Allen et al., 2014;

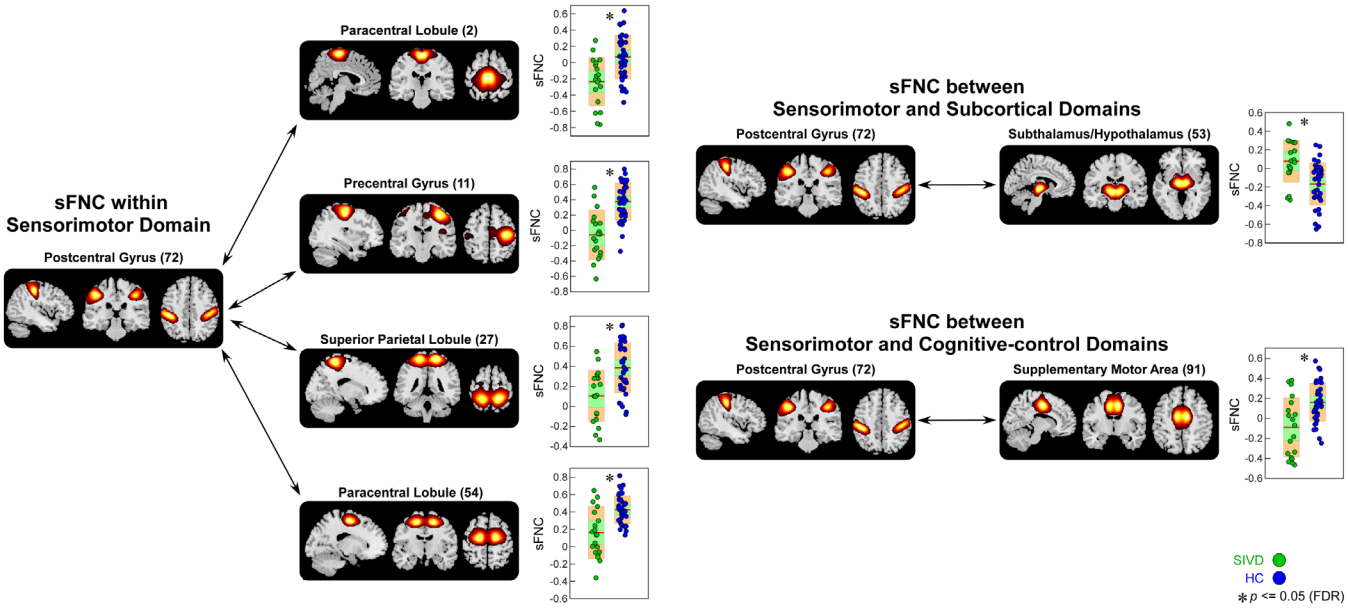

FIGURE 4 Static functional network connectivity (sFNC) significantly related to healthy control (HC)—subcortical ischemic vascular disease (SIVD) discrimination (regions involved in sensorimotor domain [SM], subcortical domain [SC], and cognitive-control domain [CC]). Boxplots of sFNC with asterisks indicating significant group difference after false discovery rate (FDR) correction [Color figure can be viewed at wileyonlinelibrary.com]

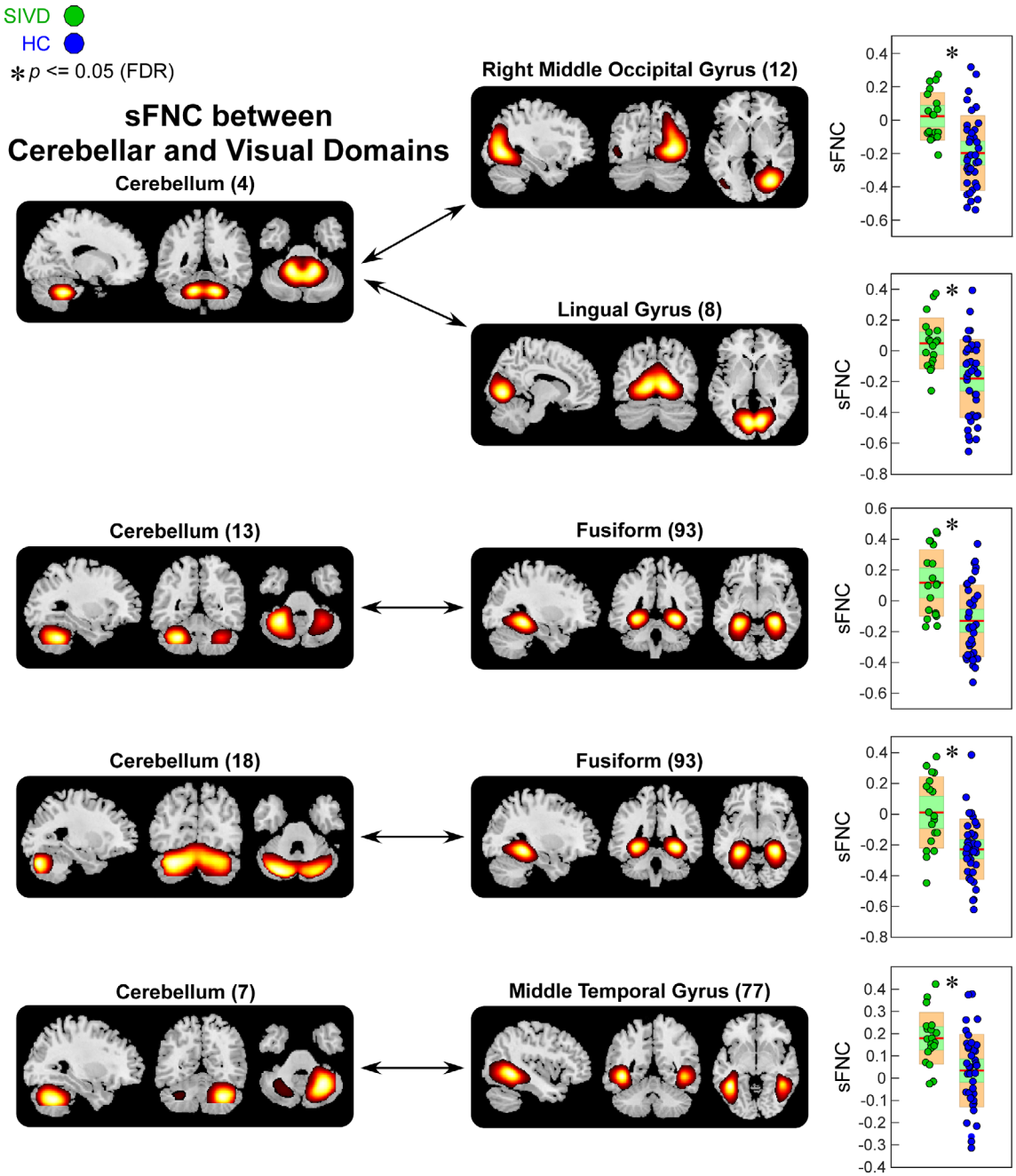

FIGURE 5 Static functional network connectivity (sFNC) significantly related to healthy control (HC)—subcortical ischemic vascular disease (SIVD) discrimination (regions involved in cerebellar domain [CB] and visual domain [VS]). Boxplots of sFNC with asterisks indicating significant group difference after false discovery rate (FDR) correction [Color figure can be viewed at wileyonlinelibrary.com]

Damaraju et al., 2014; Rashid et al., 2014), most of the subjects in the present study enter all dynamic states (for each state, subjects have at least one window assigned to. See the subject counts per state shown in Figures 9 and 10). The connectivity patterns of State 3 resemble the sFNC, which accounts for >50% of all windows. In contrast, the connectivity patterns of the other states represent connectivity diverging substantially from the sFNC. These observations are consistent with our previous longer windowed dFNC results from data with lower temporal resolutions. We highlight three differences of connectivity patterns between dFNC states, though many other distinctions can be observed. First of all, states are differentiated by DM connectivity. The ICNs within DM are highly connected in State 1, but not in the other states. States 1, 2, and 4 reveal negative correlations between DM and SM, but their connection patterns are different. Only State 2 shows positive FNC between CC and DM. Second, States 2 and 3 reveal functional segregation (even negative connectivity) between SM and VS. In contrast, SM and VS are highly connected in States 1 and 4. The third discriminating pattern among states is that, in most the states, ICNs within SM and VS show weak positive and negative correlations

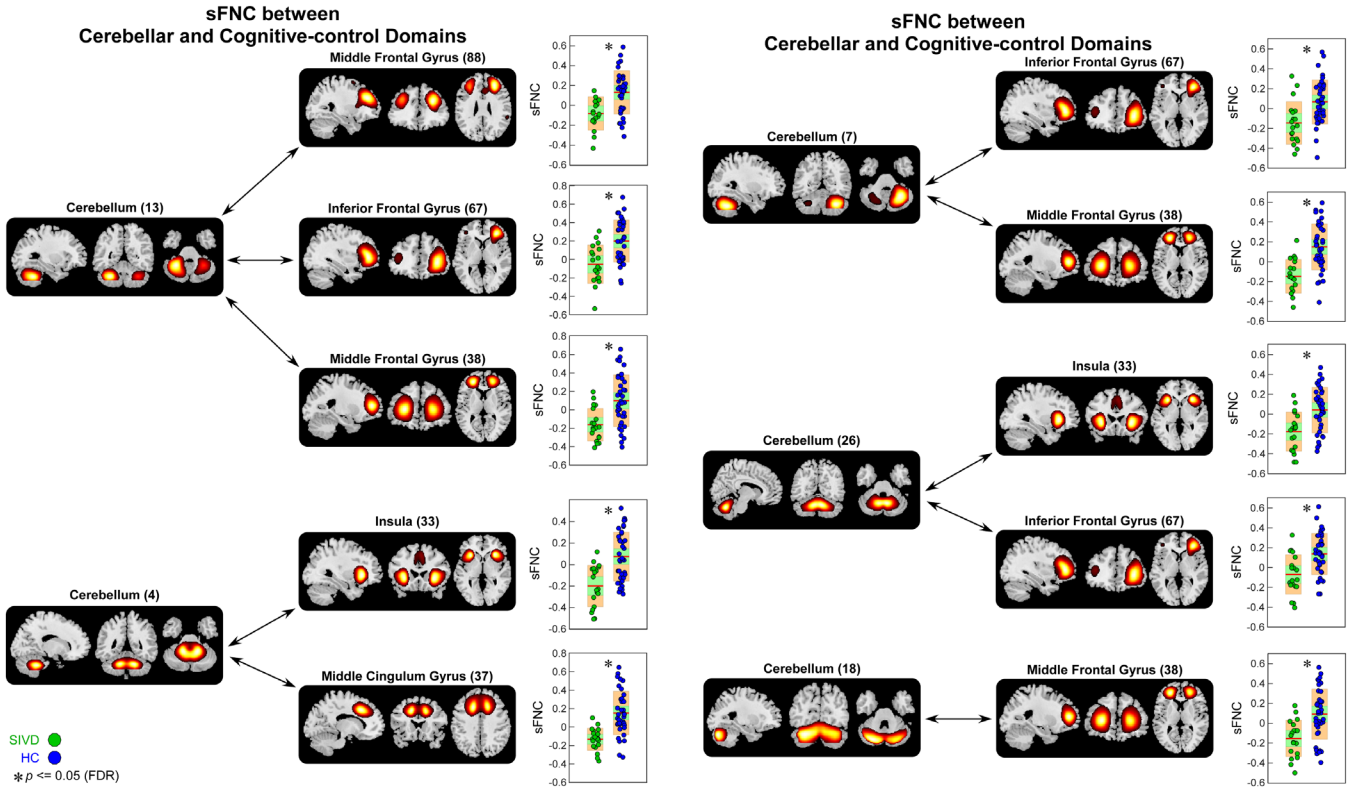

FIGURE 6 Static functional network connectivity (sFNC) significantly related to healthy control (HC)—subcortical ischemic vascular disease (SIVD) discrimination (regions involved in cerebellar domain [CB] and cognitive-control domain [CC]). Boxplots of sFNC with asterisks indicating significant group difference after false discovery rate (FDR) correction [Color figure can be viewed at wileyonlinelibrary.com]

with CB. However, in State 4, the SM and VS regions are strongly negatively correlated with many functional domains, including SC, CC, and CB.

Pair-wise group comparisons in the fraction rate of occurrences and the mean dwell time are shown in the top row of Figures 9 and 10. The results of the fraction rate indicate that patients with SIVD, in general, spend significantly more time in the relatively more sparsely connected States 2 and 3, but less time in the more positively and negatively connected States 1 and 4. Group differences can also be observed between AD and SIVD in States 1 and 3, wherein AD and

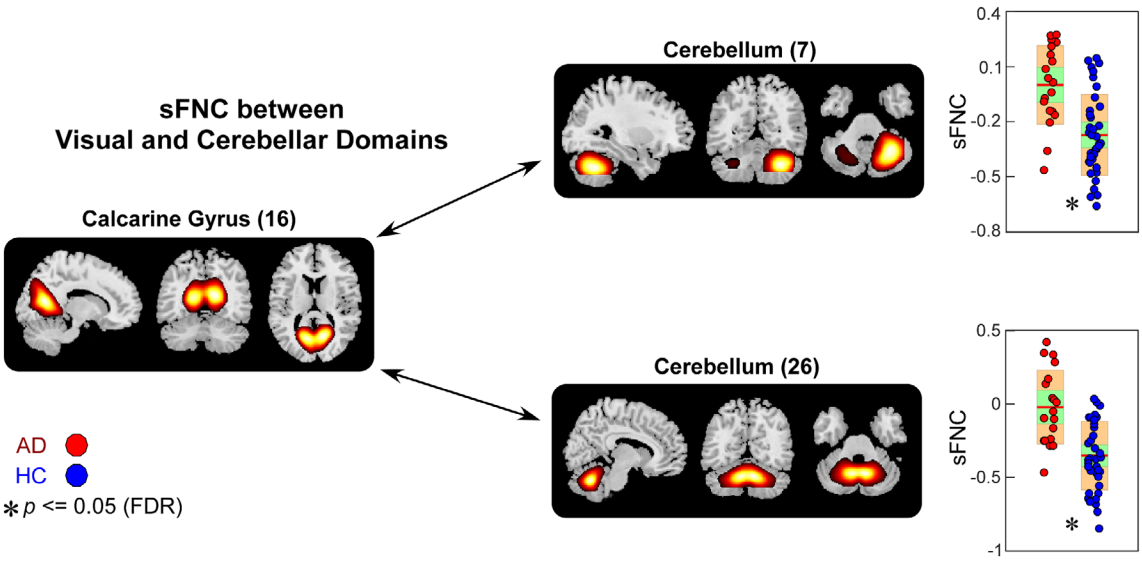

FIGURE 7 Static functional network connectivity (sFNC) significantly related to healthy control (HC)—Alzheimer's disease (AD) discrimination (regions involved in visual domain [VS] and cerebellar domain [CB]). Boxplots of sFNC with asterisks indicating significant group difference after false discovery rate (FDR) correction [Color figure can be viewed at wileyonlinelibrary.com]

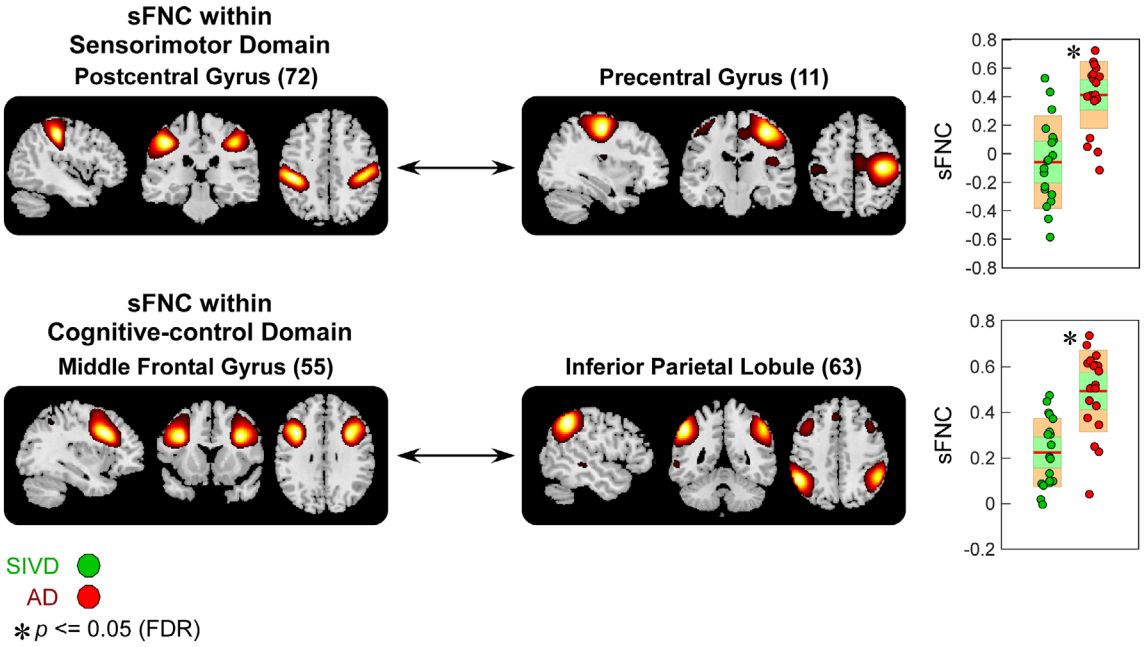

FIGURE 8 Static functional network connectivity (sFNC) significantly related to subcortical ischemic vascular disease (SIVD)—Alzheimer's disease (AD) discrimination (regions involved in sensorimotor domain [SM] and cognitive-control domain [CC]). Boxplots of sFNC with asterisks indicating significant group difference after false discovery rate (FDR) correction [Color figure can be viewed at wileyonlinelibrary.com]

SIVD show opposite alterations in the fraction rate compared with HC. AD and SIVD have similar alteration trends in States 2 and 4, but changes are much smaller in AD. The examination of the average dwell time in each state shows similar patterns that SIVD patients stay a longer time in sparsely connected State 3 and shorter time in strongly connected State 1. Interestingly, in State 2, AD shows the same alteration trend (increased mean dwell time compared with HC) as SIVD, but to a greater degree. This pattern cannot be found in the fraction rate.

3.4 | Associations between dFNC features and cognitive scores

There is a no significant association between group discriminating sFNC and cognitive scores that can pass multiple comparison correction. Figure 11 displays the results of significant associations between dFNC features and cognitive scores. In the patient groups, the fraction rate of dFNC State 2 is negatively associated with the language scores (r = –.4322, p = .0076*, q[FDR] = 0.05). The mean dwell time of State 4 is positively associated with the attention scores (r = .4729, p = .0031*, q[FDR] = 0.05) and the processing speed scores (r = .4284, p = .0082*, q[FDR] = 0.05). In the whole sample of patient plus HC groups, we found a significant association between the fraction rate of dFNC State 2 and the language score (r = –.3660, p = .0013*, q[FDR] = 0.05), which is consistent with the observations in the patient group. Even when we regressed out the label effects, most of the identified associations are still significant (FDR corrected, q = 0.05). An exception is the association between the fraction rate of dFNC State 2 and the language score in the whole sample, which shows a similar trend with boundary significance (r = –.2861, p = .0135, uncorrected).

4 | DISCUSSION

The present work employed both sFNC analysis and dFNC analysis to clarify rs-FC changes in AD and SIVD, and we further explored the potential association between rs-FC changes and cognitive impairment. Our results highlight that: (a) AD patients and SIVD patients have common and specific sFNC changes, (b) AD patients and SIVD patients share similar and opposite alteration trends in dFNC, and (c) dFNC is more sensitive to the cognitive performance as measured with the neuropsychological scores. The overall findings suggest that the dFNC analysis can provide additional relevant information on diseases beyond the static parts. Investigating rs-FC from both static and dynamic perspective can help to depict a full picture of rs-FC abnormalities related to brain disorders.

4.1 | Static FNC abnormalities in AD and SIVD

Relative to HCs, the PoCG in patients with SIVD shows significantly decreased sFNC with five cortical ICNs, most of which located in the SM domain (including ParaCL, PreCG, and SPL). Our results concur with previous studies in VCID and WMHs that reported decreased rs-FC involving the parietal cortex (Ding et al., 2017; Sang et al., 2018; Sun et al., 2011; Zhang et al., 2013). Parietal cortex includes a set of important brain areas that are responsible for integrating sensory information, especially for language processing. Considering that a decline of language processing is a common symptom in SIVD, a

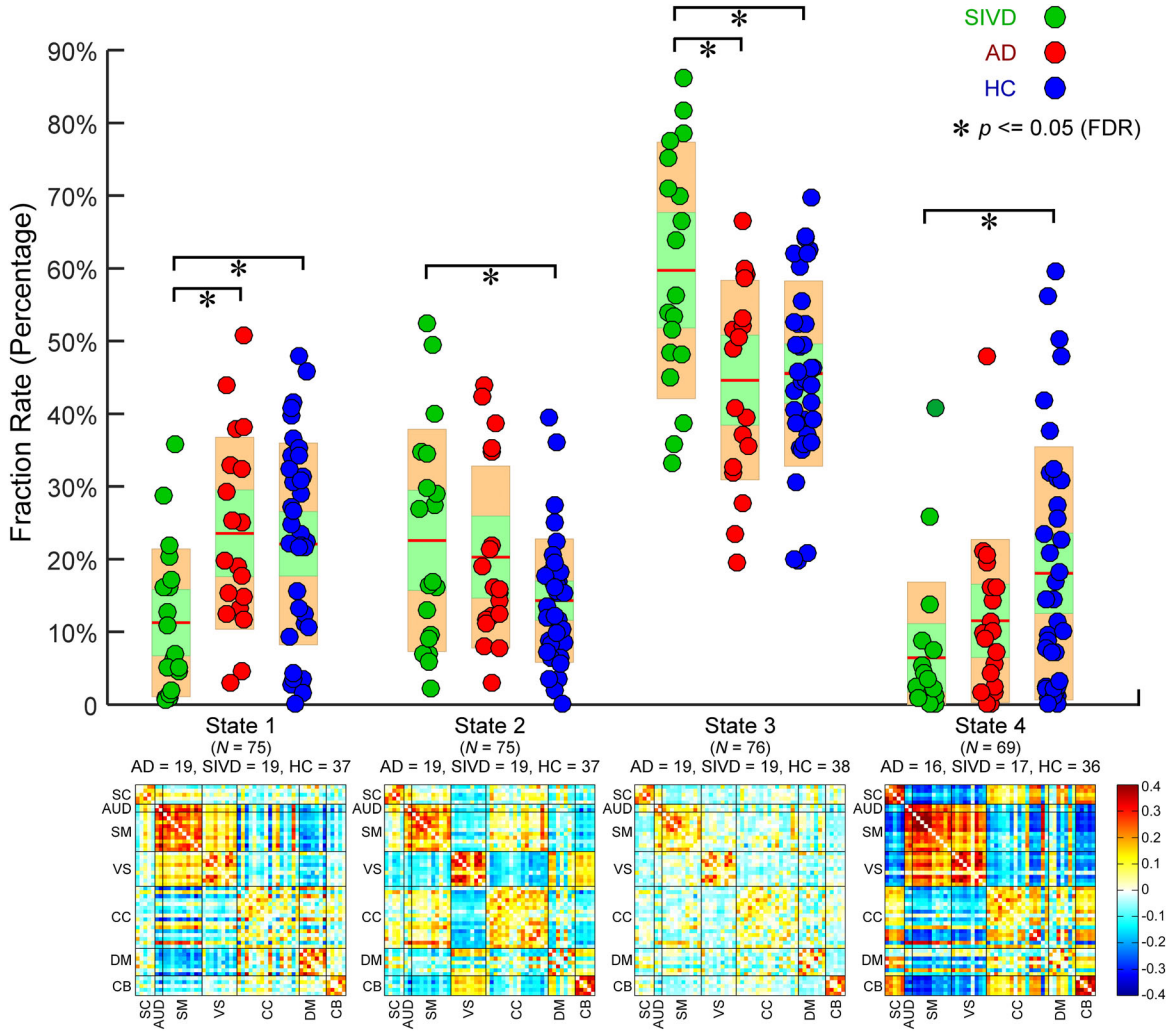

FIGURE 9 Upper: Group comparisons in fraction rate of occurrences of four dynamic functional network connectivity (dFNC) states. Boxplots of fraction rate of occurrences with asterisks indicating significant group difference after false discovery rate (FDR) correction. Lower: The cluster centroids of four dFNC states, along with the count of subjects that have at least one window clustered into each state [Color figure can be viewed at wileyonlinelibrary.com]

growing literature has suggested relating the disrupted connectivity in the parietal cortex to such cognitive impairment in SIVD. Previous studies further identified decreased nodal efficiency and clustering coefficient in the parietal areas, implying that the decreased FC in parietal cortex might result in their lower capacity for information exchange, which can influence the response to noncognitive consequences and motor dysfunction in patients with cognitive impairment caused by SIVD (Gupta et al., 2014; Lyketsos et al., 2002). SIVD patients also show increased sFNC between thalamus/hypothalamus and PoCG and such thalamocortical connectivity changes have been widely reported in many other brain disorders (Cerliani et al., 2015; Damaraju et al., 2014; Fu et al., 2018). The observation of SC–cortical hyperconnectivity targeting the sensory cortices might help to conceptualize the presence of sensory abnormalities in SIVD. In most of the clinical literature, the sensory deficit and pure sensory loss are key criteria for the diagnosis of SIVD (Alves et al., 2009; Chui, 2007; Román et al., 2002b). Our results suggest that the presence of atypical sensory processing in SIVD might result in a compensation mechanism of the information flow from thalamic nuclei to the cortex, reflected indirectly by our findings of thalamo-sensory hyperconnectivity.

In our study, atypical CB sFNC is identified in both dementia patient groups, where such abnormalities are relatively weaker in the AD patients. Although the cerebellum is traditionally supposed to be related to motor behavior, recent evidence has argued that the cerebellum acts as a center that subserves multiple cognitive functions by connecting to distributed networks and facilitating their modulation (O'reilly, Beckmann, Tomassini, Ramnani, & Johansen-Berg 2009; Schmahmann, 2018; Schmahmann, Weilburg, & Sherman, 2007). For example, the cerebellum has been shown to be associated with the memory function (Jantzen, Oullier, Marshall, Steinberg, & Kelso, 2007; Ng et al., 2016). Literature has identified numerous CB abnormalities in different types of dementia, such as the atypical CB connectivity in both AD (Castellazzi et al., 2014; Zheng et al., 2017) and SIVD (Cheng et al., 2017; Diciotti et al., 2017; Ding et al., 2017). However, the results of atypical CB

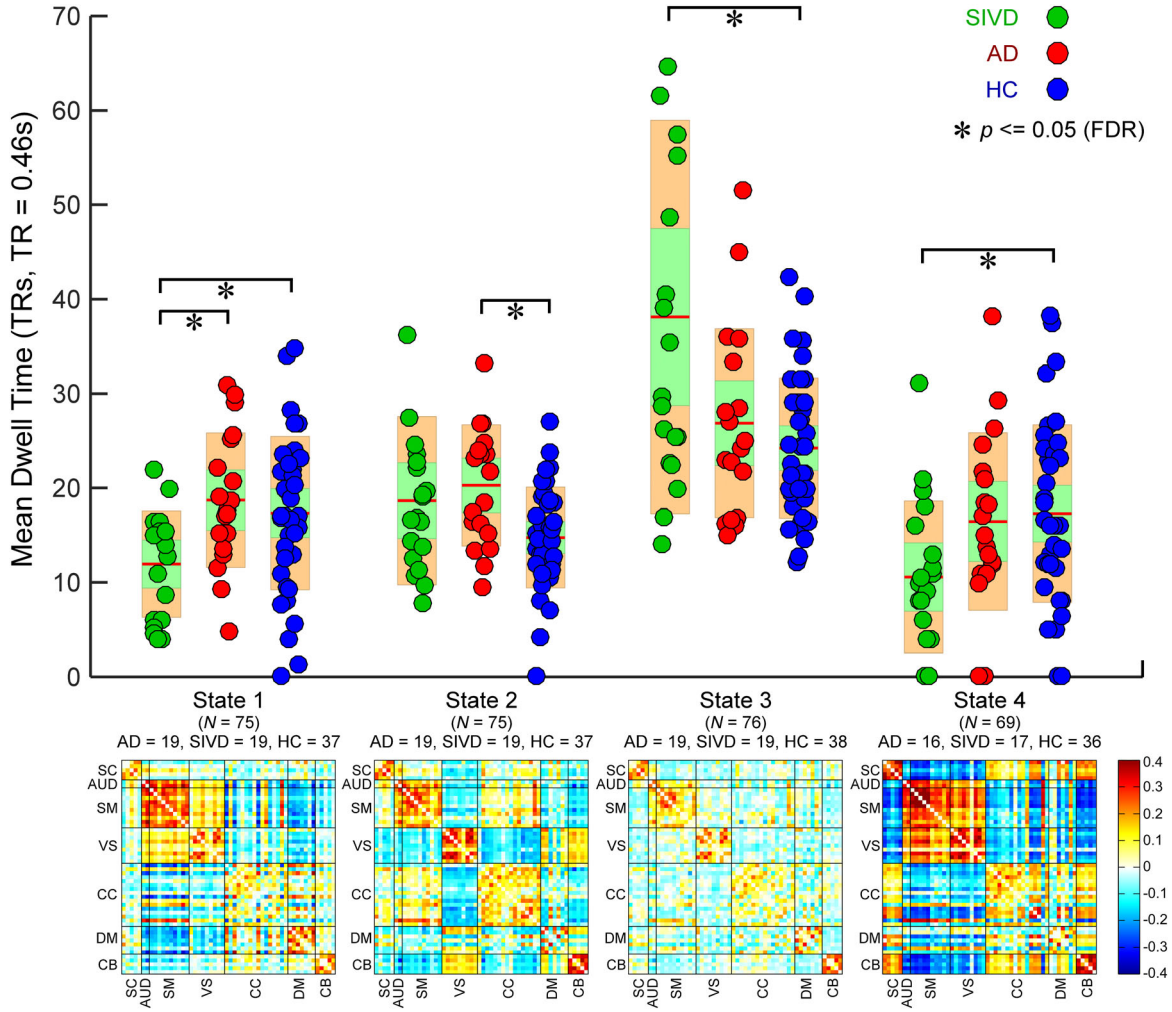

FIGURE 10 Upper: Group comparisons in mean dwell time of four dynamic functional network connectivity (dFNC) states. Boxplots of mean dwell time with asterisks indicating significant group difference after false discovery rate (FDR) correction. Lower: The cluster centroids of four dFNC states, along with the count of subjects that have at least one window clustered into each state [Color figure can be viewed at wileyonlinelibrary.com]

connectivity are not so consistent, since both hypoconnectivity and hyperconnectivity are observed across different studies. With the help of a high model order group ICA, we parcellated the whole brain into more functional regions and successfully identified both increased and decreased CB connectivity in the same discovery data set. Our results show that the connectivity between the cerebellum and primary sensory cortex generally increases, while the connectivity between the cerebellum and frontal cortex generally decreases in patients with dementia. This suggests the definition of the regions of interest to be a possible source of previous disparities. The identified hypoconnectivity involved in the frontal cortex is also in line with previous studies (Sang et al., 2018; Zhou et al., 2016). Our results show that SIVD has larger alterations in frontal connectivity than AD. Volume atrophy and cortical thinning in the frontal cortex have been widely observed in SIVD patients (Jin Thong et al., 2014; Seo et al., 2010). Widespread WM lesions in SIVD are also suggested to have effects on frontal function due to the disruption of long-range association fibers (Aralasmak et al., 2006; Chui, 2007). Considering the potential associations between structural and functional abnormalities (Sui et al., 2011; Sui et al., 2015), we argue that the lesions of brain structure, especially in WM, would be the cause of more severe frontal connectivity abnormalities in SIVD. Interestingly, we found that although either AD or SIVD does not have significantly different FNC between MiFG and IPL compared with HCs, this FNC shows a significant difference between AD and SIVD, indicating opposite alterations (increased in AD but decreased in SIVD) across patient groups. Such differences suggest that dysfunction in AD and SIVD could stem from distinct changes on the information processing in the brain underlying disparate gray matter damages. The increased FNC in AD might support the hypothesis that AD patients recruit more resources in the prefrontal cortex to compensate for cognitive function loss (Grady et al., 2003). In contrast, the decreased FNC in SIVD might be attributed to the disruption of frontal circuits (relevant to executive function, initiation, and social behavior) and the softening of the WM in the frontal lobe (Cummings, 1993; Dozono, Ishii, Nishihara, & Horie, 1991).

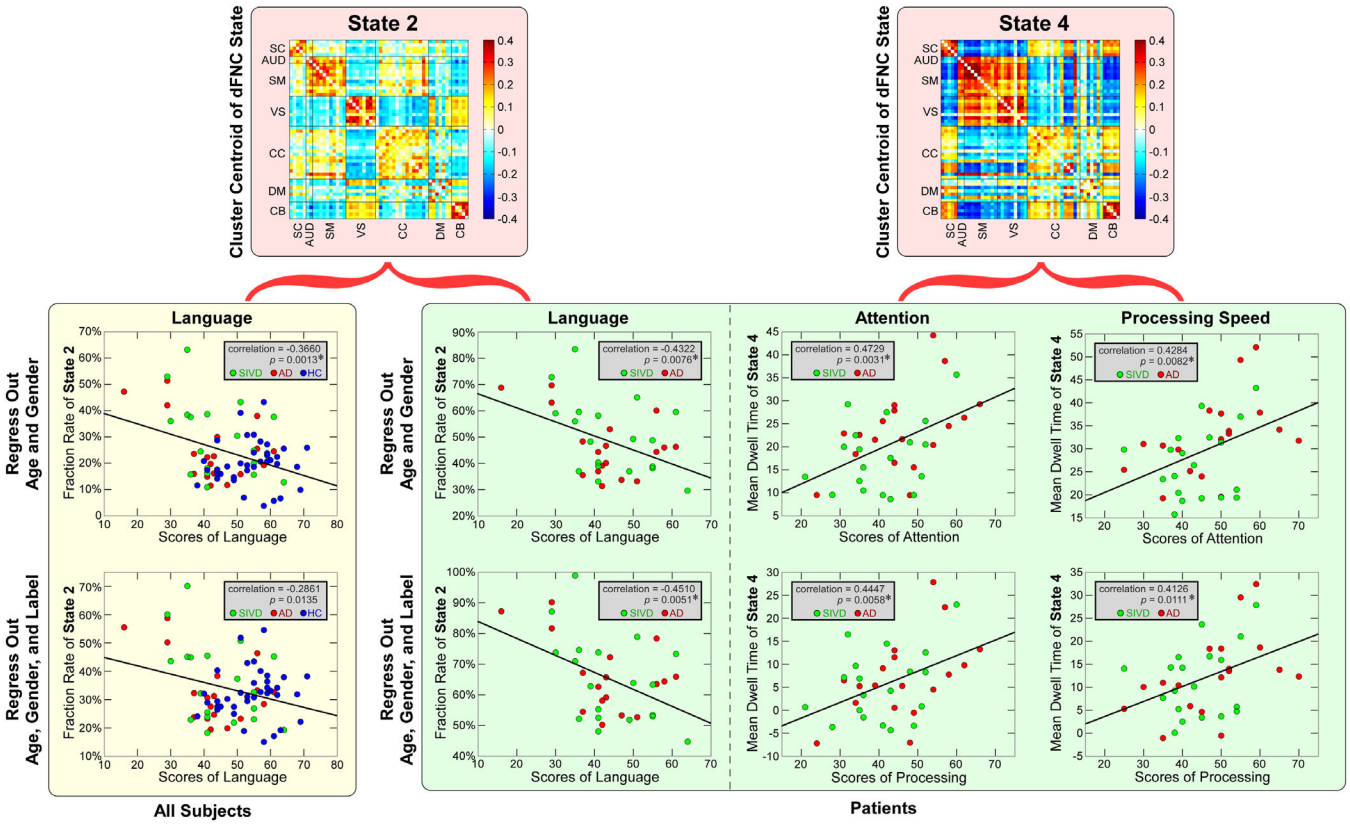

FIGURE 11 The scatterplots illustrate the associations between cognitive scores and each dynamic functional network connectivity (dFNC) feature in the whole samples and in the patient groups. Green circles represent the patients with subcortical ischemic vascular disease (SIVD), red circles represent the patients with Alzheimer's disease (AD), and blue circles represent the healthy controls (HCs). Significant correlations are indicated by asterisks (false discovery rate [FDR] corrected, $q = 0.05$) [Color figure can be viewed at wileyonlinelibrary.com]

4.2 | Dynamic FNC abnormalities and its associations with cognitive impairment

In this work, a sliding window approach with relatively shorter window size (around 10 s) was applied on a high temporal resolution data set for the exploration of atypical dFNC in different types of dementia. Although the selected window size is much smaller than that used in prior literature (Allen et al., 2014; Marusak et al., 2017), we could still identify highly reproducible dFNC states in AD and SIVD, which are similar to previous findings in other brain disorders (Damaraju et al., 2014; Kim et al., 2017; Rashid et al., 2014; Rashid et al., 2016). The highly variable dFNC patterns among different states depart significantly from the sFNC patterns, which imply the flexibility in functional coordination between brain subsystems (Allen et al., 2014; Marusak et al., 2017). For example, the auditory, SM, and VSs exhibited strongly synchronous activity and antagonism with SC simultaneously only in State 4. Literature has shown these connectivity patterns to be associated with the electroencephalography (EEG) oscillations in simultaneous EEG–fMRI recordings (Allen et al., 2018). The most frequently reoccurring State 3 has the weak connectivity patterns that resembled the sFNC patterns. In previous dFNC studies, a dynamic state that resembles the stationary FNC patterns typically accounts for the largest percentage of windows. It is speculated that such a weak and diffused dynamic state represents the average of a large number of additional states with less variability to be separated (Allen et al., 2014). Recent studies further show that this state might be associated with self-referential processing and drowsiness based on a greater frequency of occurrence over time and temporal similarity across groups (Allen et al., 2018; Marusak et al., 2017). Taken together, this dynamic state could be considered as a more steady state with reduced vigilance. It signifies the average of less variable FNC, sharing similar stationary assumption and connectivity patterns with the sFNC. Some other states (States 1 and 2) show similar within-domain connectivity patterns with State 3, but with different negative between-domains connectivity patterns.

HCs and dementia patients showed different fraction rates of occurrences in different dFNC states. More specifically, relative to HCs, SIVD patients spend less time in strongly connected states with antagonism connectivity patterns (States 1 and 4). AD patients show a similar decreasing trend in State 4. We speculate that the decrease in the occurrence of these states will result in disrupting functional segregation, which is further linked to the cognitive decline in dementia (Sang et al., 2018; Yu et al., 2015). SIVD patients also have more occurrences in the weak connected states, especially in the state that resembles the sFNC (State 3). Similar observations can be found in many other brain disorders, such as bipolar disorder (Rashid et al., 2014), schizophrenia (Damaraju et al., 2014), autism (Fu et al., 2018), and Parkinson (Kim et al., 2017). However, it is interesting to note

that, different from SIVD, AD patients do not exhibit such atypical patterns in the occurrence of State 3. Our results suggest that such abnormalities in dFNC might underlie similar dysfunctions across different brain disorders, except for AD, which might have different pathology compared with the others. AD and SIVD have similar changes in dynamic features of State 2, but their alteration levels are different. AD has more increase in mean dwell time of State 2, but less increase in the occurrence of State 2 than SIVD. We speculate that AD and SIVD might have different dynamic behaviors. Specifically, AD would spend significantly longer duration in State 2, while SIVD would enter into State 2 more frequently. The investigation of dynamic brain connectivity might help to capture AD- and SIVD-related impairments in transient brain organization that cannot be observed from the static analysis.

Significant associations are identified between dFNC features (fraction rate of occurrences and mean dwell time) and cognitive performance indexed by neuropsychological scores. Importantly, these associations cannot be observed between sFNC features and the same cognitive scores. These findings, together with previous research on other psychiatric disorders (Du et al., 2018; Fu et al., 2018), highlight the importance of evaluating dynamic connectivity for tracking the cognitive declines and disease traits. Our results unveil a relationship between language performance and the fraction rate of dFNC State 2, where the few occurrences indicate better language performance. The language dysfunction, including both comprehension and production, is a hallmark symptom in different types of dementia (Brotons & Koger, 2000; Potkins et al., 2003) and might also reflect the overall severity of dementia (Morris, 1997). A system of regions are involved in language function, including the frontal cortex, temporal cortex, and parietal cortex, most of which are mainly located in sensory networks and CC network (Friederici et al., 2013; Gow Jr, 2012; Hickok & Poeppel, 2007). In most of the dFNC states identified in our current study, the sensory domains (auditory, SM, and VSs) work homogeneously with the CC domain, as represented by similar negative relationships between sensory domains and CC domain. However, in State 2, those sensory domains show different functional relationships with the CC domain, where the CC domain is positively correlated with the auditory and SM domains and negatively correlated with the VS. This "heterogeneous state" might imply a loss of cooperation in those language-related regions, and we argue that greater occurrences into this state would result in a drop of language performance. We also found positive associations between the mean dwell time of State 4 and scores of attention, as well as processing speed, in the patient groups. Attention and information-processing deficits are two common syndromes in AD and SIVD (Loring, Meador, Mahurin, & Largen, 1986; Mazzucchi et al., 1987). Literature has shown that poorer attention and information-processing performance might reflect a greater pathology in the frontal cortex and more corticocortical disconnection in dementia (Perry & Hodges, 1999). Our results are in line with this previous finding to some extent by showing that the patients spending a longer time in a dFNC state with strongly connected patterns would have better performance in attention and processing speed. The positive correlation between the mean dwell time of State 4 and attention scores also implies potential relationships between DM impairments and attention deficits. DM regions play a critical role in regulating the focus of attention (Raichle et al., 2001) and are suggested to be associated with attention deficits (Bonnelle et al., 2011). Precuneus is a major DM region, whose impairments have been widely reported in different types of dementia, including reduced precuneus connectivity (Zang, Jiang, Lu, He, & Tian, 2004; Zhang et al., 2009) and precuneus atrophy (Karas et al., 2007). Our clustering results show that State 4 has relatively stronger connectivity between precuneus and sensory regions than the other states. We speculate that less time spent in this state would influence the information exchange between precuneus and sensory regions and such disruption in the precuneus–sensory interactions might ultimately result in attention deficits in dementia (Kim, Kim, & Lee, 2013).

4.3 | Limitations and future directions

The present study has explored atypical brain connectivity using the data set scanned with two different head coils. The resulting data set thus has different temporal resolutions (TR = 0.46 s and TR = 2 s), which might introduce potential confounding effects on the connectivity features. Therefore, we applied a GLM method for removing the head coil effect from the sFNC and dFNC estimates, respectively, before the statistical analysis. For the dFNC analysis, we also did interpolation on the estimates with the lower temporal resolution to reduce the head coil difference. However, it is still not clear whether this head coil difference influences the connectivity, especially the dFNC, which are estimated using the localized data set (with fewer observations) and thus are more sensitive to the temporal resolution. In future studies with more scans having the same temporal resolution (our ongoing VCID study is now only collecting data set using the 32-channel RF coil), we can validate our current findings using only subjects with the same TR. Also due to the limited number of subjects, we did not have enough power to investigate associations between FNC features and cognitive scores for each group separately. We investigated associations between dFNC features and cognitive scores for each patient group using the same GLM analysis and the results show similar associations between dFNC features and cognitive scores but with relatively weaker significance ($p \leq .05$, uncorrected or near significance. Results are provided in Appendix S1). With more scans collected in the future, we can investigate such associations for each group, respectively, and determine whether such associations change across patient groups.

Another potential issue is the window size selection in the estimation of dFNC. Although we found highly consistent cluster centroids (from 16 to 24 TRs) that are similar to or even better than (because unlike previous studies, most of the subjects in our study can have at least one window assigned to every centroid) those identified in previous work (Allen et al., 2014; Du et al., 2018; Rashid et al., 2014), it is still challenging using such a short window size for the dFNC estimation. Previous dynamic connectivity studies generally employed a window size within the range of 30–60 s (around 15–30 TRs) for the

sliding window estimation, which is considered as a reasonable choice for capturing the real variations in the brain connectivity (Allen et al., 2014; Hutchison, Womelsdorf, Allen, et al., 2013a; Hutchison, Womelsdorf, Gati, et al., 2013b; Zalesky, Fornito, Cocchi, Gollo, & Breakspear, 2014). We argue that such a window size selection is just due to the limitation of the low temporal resolution of the fMRI data. Traditional fMRI data sets typically have the TR around 2 s. In that case, the window size could not be too short (e.g., <10 s), in that there might not be enough observations to guarantee the estimation accuracy of dynamic connectivity. Research using high-temporal-resolution imaging techniques (such as EEG) has identified reoccurring microstates related to spontaneous thoughts and mental processes in a much shorter temporal scale (Lehmann, Strik, Henggeler, König, & Koukkou, 1998). This suggests that the resting-state brain connectivity could have high-frequency fluctuations that might be overly smoothed out by using a long window size. The results of this study show that employing sliding window approaches with short window size (around 10 s) on high temporal resolution fMRI data can capture more transient dynamics in functional connectivity and thus identify more robust connectivity states. Additional experiments are still needed, such as a comprehensive simulation study and the simultaneous EEG-high temporal resolution fMRI studies, for unveiling the relationship between the dFNC and the real dynamics in the mental activities. This will help us determine the optimal window size for capturing brain connectivity dynamics.

ACKNOWLEDGMENTS

This work is supported by the National Institutes of Health (NIH) grants (1UH2NS100598-01, PI: G.A.R.; R01EB006841, R01REB020407, and P20GM103472, PI: V.D.C.).

ORCID

Zening Fu https://orcid.org/0000-0002-1591-4900
Yuhui Du https://orcid.org/0000-0002-0079-8177
Jing Sui https://orcid.org/0000-0001-6837-5966

REFERENCES

Agosta, F., Pievani, M., Geroldi, C., Copetti, M., Frisoni, G. B., & Filippi, M. (2012). Resting state fMRI in Alzheimer's disease: Beyond the default mode network. *Neurobiology of Aging*, *33*, 1564–1578. https://doi.org/10.1016/j.neurobiolaging.2011.06.007

Allen, E. A., Damaraju, E., Eichele, T., Wu, L., & Calhoun, V. D. (2018). EEG signatures of dynamic functional network connectivity states. *Brain Topography*, *31*, 101–116. https://doi.org/10.1007/s10548-017-0546-2

Allen, E. A., Damaraju, E., Plis, S. M., Erhardt, E. B., Eichele, T., & Calhoun, V. D. (2014). Tracking whole-brain connectivity dynamics in the resting state. *Cerebral Cortex*, *24*, 663–676. https://doi.org/10.1093/cercor/bhs352

Alves, G. S., Alves, C. E. D. O., Lanna, M. E. D. O., Ericeira-Valente, L., Sudo, F. K., Moreira, D., … Laks, J. (2009). Clinical characteristics in subcortical ischemic white matter disease. *Arquivos de Neuro-Psiquiatria*, *67*, 173–178. https://doi.org/10.1590/S0004-282X2009000200001

Anastasi, A., & Urbina, S. (1997). *Psychological testing*. Upper Saddle River, NJ, US: Prentice Hall/Pearson Education.

Andersson, J. L., Skare, S., & Ashburner, J. (2003). How to correct susceptibility distortions in spin-echo echo-planar images: Application to diffusion tensor imaging. *NeuroImage*, *20*, 870–888. https://doi.org/10.1016/S1053-8119(03)00336-7

Aralasmak, A., Ulmer, J. L., Kocak, M., Salvan, C. V., Hillis, A. E., & Yousem, D. M. (2006). Association, commissural, and projection pathways and their functional deficit reported in literature. *Journal of Computer Assisted Tomography*, *30*, 695–715. https://doi.org/10.1097/01.rct.0000226397.43235.8b

Badhwar, A., Tam, A., Dansereau, C., Orban, P., Hoffstaedter, F., & Bellec, P. (2017). Resting-state network dysfunction in Alzheimer's disease: A systematic review and meta-analysis. *Alzheimer's & Dementia: Diagnosis, Assessment & Disease Monitoring*, *8*, 73–85. https://doi.org/10.1016/j.dadm.2017.03.007

Benjamini, Y., & Hochberg, Y. (1995). Controlling the false discovery rate: A practical and powerful approach to multiple testing. *Journal of the Royal Statistical Society. Series B (Methodological)*, *57*, 289–300. https://doi.org/10.2307/2346101

Binnewijzend, M. A., Schoonheim, M. M., Sanz-Arigita, E., Wink, A. M., van der Flier, W. M., Tolboom, N., … van Berckel, B. N. (2012). Resting-state fMRI changes in Alzheimer's disease and mild cognitive impairment. *Neurobiology of Aging*, *33*, 2018–2028. https://doi.org/10.1016/j.neurobiolaging.2011.07.003

Biswal, B., Zerrin Yetkin, F., Haughton, V. M., & Hyde, J. S. (1995). Functional connectivity in the motor cortex of resting human brain using echo-planar MRI. *Magnetic Resonance in Medicine*, *34*, 537–541. https://doi.org/10.1002/mrm.1910340409

Bondi, M. W., Edmonds, E. C., Jak, A. J., Clark, L. R., Delano-Wood, L., McDonald, C. R., … Galasko, D. (2014). Neuropsychological criteria for mild cognitive impairment improves diagnostic precision, biomarker associations, and progression rates. *Journal of Alzheimer's Disease*, *42*, 275–289. https://doi.org/10.3233/JAD-140276

Bonnelle, V., Leech, R., Kinnunen, K. M., Ham, T. E., Beckmann, C. F., De Boissezon, X., … Sharp, D. J. (2011). Default mode network connectivity predicts sustained attention deficits after traumatic brain injury. *Journal of Neuroscience*, *31*, 13442–13451. https://doi.org/10.1523/JNEUROSCI.1163-11.2011

Brotons, M., & Koger, S. M. (2000). The impact of music therapy on language functioning in dementia. *Journal of Music Therapy*, *37*, 183–195. https://doi.org/10.1093/jmt/37.3.183

Calhoun, V. D., & Adali, T. (2012). Multisubject independent component analysis of fMRI: A decade of intrinsic networks, default mode, and neurodiagnostic discovery. *IEEE Reviews in Biomedical Engineering*, *5*, 60–73. https://doi.org/10.1109/RBME.2012.2211076

Calhoun, V. D., Adali, T., Pearlson, G. D., & Pekar, J. (2001). A method for making group inferences from functional MRI data using independent component analysis. *Human Brain Mapping*, *14*, 140–151. https://doi.org/10.1002/Hbm.1048

Calhoun, V. D., Miller, R., Pearlson, G., & Adalı, T. (2014). The chronnectome: Time-varying connectivity networks as the next frontier in fMRI data discovery. *Neuron*, *84*, 262–274. https://doi.org/10.1016/j.neuron.2014.10.015

Castellazzi, G., Palesi, F., Casali, S., Vitali, P., Sinforiani, E., Wheeler-Kingshott, C. A., & D'Angelo, E. (2014). A comprehensive assessment of resting state networks: Bidirectional modification of functional integrity in cerebro-cerebellar networks in dementia. *Frontiers in Neuroscience*, *8*, 223. https://doi.org/10.3389/fnins.2014.00223

Cerliani, L., Mennes, M., Thomas, R. M., Di Martino, A., Thioux, M., & Keysers, C. (2015). Increased functional connectivity between subcortical and cortical resting-state networks in autism spectrum

disorder. *JAMA Psychiatry*, *72*, 767–777. https://doi.org/10.1001/jamapsychiatry.2015.0101

Chang, C., & Glover, G. H. (2010). Time–frequency dynamics of resting-state brain connectivity measured with fMRI. *NeuroImage*, *50*, 81–98. https://doi.org/10.1016/j.neuroimage.2009.12.011

Cheng, R., Qi, H., Liu, Y., Zhao, S., Li, C., Liu, C., & Zheng, J. (2017). Abnormal amplitude of low-frequency fluctuations and functional connectivity of resting-state functional magnetic resonance imaging in patients with leukoaraiosis. *Brain and Behavior*, *7*, e00714. https://doi.org/10.1002/brb3.714

Chui, H. C. (2007). Subcortical ischemic vascular dementia. *Neurologic Clinics*, *25*, 717–740. https://doi.org/10.1016/j.ncl.2007.04.003

Cordes, D., Haughton, V. M., Arfanakis, K., Carew, J. D., Turski, P. A., Moritz, C. H., … Meyerand, M. E. (2001). Frequencies contributing to functional connectivity in the cerebral cortex in "resting-state" data. *American Journal of Neuroradiology*, *22*, 1326–1333.

Corriveau, R. A., Bosetti, F., Emr, M., Gladman, J. T., Koenig, J. I., Moy, C. S., … Koroshetz, W. (2016). The science of vascular contributions to cognitive impairment and dementia (VCID): A framework for advancing research priorities in the cerebrovascular biology of cognitive decline. *Cellular and Molecular Neurobiology*, *36*, 281–288. https://doi.org/10.1007/s10571-016-0334-7

Cummings, J. L. (1993). Frontal-subcortical circuits and human behavior. *Archives of Neurology*, *50*, 873–880.

Dai, Z., Yan, C., Wang, Z., Wang, J., Xia, M., Li, K., & He, Y. (2012). Discriminative analysis of early Alzheimer's disease using multi-modal imaging and multi-level characterization with multi-classifier (M3). *NeuroImage*, *59*, 2187–2195. https://doi.org/10.1016/j.neuroimage.2011.10.003

Damaraju, E., Allen, E., Belger, A., Ford, J., McEwen, S., Mathalon, D., … Preda, A. (2014). Dynamic functional connectivity analysis reveals transient states of dysconnectivity in schizophrenia. *NeuroImage: Clinical*, *5*, 298–308. https://doi.org/10.1016/j.nicl.2014.07.003

de Lacy, N., Doherty, D., King, B., Rachakonda, S., & Calhoun, V. D. (2017). Disruption to control network function correlates with altered dynamic connectivity in the wider autism spectrum. *NeuroImage: Clinical*, *15*, 513–524. https://doi.org/10.1016/j.nicl.2017.05.024

de Vos, F., Koini, M., Schouten, T. M., Seiler, S., van der Grond, J., Lechner, A., … Rombouts, S. A. (2018). A comprehensive analysis of resting state fMRI measures to classify individual patients with Alzheimer's disease. *NeuroImage*, *167*, 62–72. https://doi.org/10.1016/j.neuroimage.2017.11.025

Diciotti, S., Orsolini, S., Salvadori, E., Giorgio, A., Toschi, N., Ciulli, S., … Pantoni, L. (2017). Resting state fMRI regional homogeneity correlates with cognition measures in subcortical vascular cognitive impairment. *Journal of the Neurological Sciences*, *373*, 1–6. https://doi.org/10.1016/j.jns.2016.12.003

Ding, X., Ding, J., Hua, B., Xiong, X., Xiao, L., Peng, F., … Wang, Q. (2017). Abnormal cortical functional activity in patients with ischemic white matter lesions: A resting-state functional magnetic resonance imaging study. *Neuroscience Letters*, *644*, 10–17. https://doi.org/10.1016/j.neulet.2017.02.015

Dozono, K., Ishii, N., Nishihara, Y., & Horie, A. (1991). An autopsy study of the incidence of lacunes in relation to age, hypertension, and arteriosclerosis. *Stroke*, *22*, 993–996. https://doi.org/10.1161/01.str.22.8.993

Du, Y., Allen, E. A., He, H., Sui, J., Wu, L., & Calhoun, V. D. (2016a). Artifact removal in the context of group ICA: A comparison of single-subject and group approaches. *Human Brain Mapping*, *37*, 1005–1025. https://doi.org/10.1002/hbm.23086

Du, Y., & Fan, Y. (2013). Group information guided ICA for fMRI data analysis. *NeuroImage*, *69*, 157–197. https://doi.org/10.1016/j.neuroimage.2012.11.008

Du, Y., Fryer, S. L., Fu, Z., Lin, D., Sui, J., Chen, J., … Calhoun, V. D. (2018). Dynamic functional connectivity impairments in early schizophrenia and clinical high-risk for psychosis. *NeuroImage*, *180*, 632–645. https://doi.org/10.1016/j.neuroimage.2017.10.022

Du, Y., Pearlson, G. D., Lin, D., Sui, J., Chen, J., Salman, M., … Keshavan, M. S. (2017). Identifying dynamic functional connectivity biomarkers using GIG-ICA: Application to schizophrenia, schizoaffective disorder, and psychotic bipolar disorder. *Human Brain Mapping*, *38*, 2683–2708. https://doi.org/10.1002/hbm.23553

Du, Y., Pearlson, G. D., Yu, Q., He, H., Lin, D., Sui, J., … Calhoun, V. D. (2016b). Interaction among subsystems within default mode network diminished in schizophrenia patients: A dynamic connectivity approach. *Schizophrenia Research*, *170*, 55–65. https://doi.org/10.1016/j.schres.2015.11.021

Erhardt, E., Pesko, J. C., Prestopnik, J., Thompson, J., Caprihan, A., & Rosenberg, G. A. (2018). Biomarkers identify the Binswanger type of vascular cognitive impairment. *Journal of Cerebral Blood Flow & Metabolism*. 0271678X18762655. https://doi.org/10.1177/0271678X18762655

Ferman, T. J., Smith, G. E., Kantarci, K., Boeve, B. F., Pankratz, V. S., Dickson, D. W., … Uitti, R. (2013). Nonamnestic mild cognitive impairment progresses to dementia with Lewy bodies. *Neurology*, *81*, 2032–2038. https://doi.org/10.1212/01.wnl.0000436942.55281.47

Friederici, A. D., & Gierhan, S. M. (2013). The language network. *Current Opinion in Neurobiology*, *23*, 250–254. https://doi.org/10.1016/j.conb.2012.10.002

Friedman, J., Hastie, T., & Tibshirani, R. (2008). Sparse inverse covariance estimation with the graphical lasso. *Biostatistics*, *9*, 432–441. https://doi.org/10.1093/biostatistics/kxm045

Fu, Z., Tu, Y., Di, X., Du, Y., Pearlson, G., Turner, J., … Calhoun, V. (2017). Characterizing dynamic amplitude of low-frequency fluctuation and its relationship with dynamic functional connectivity: An application to schizophrenia. *NeuroImage*, *180*, 619–631. https://doi.org/10.1016/j.neuroimage.2017.09.035

Fu, Z., Tu, Y., Di, X., Du, Y., Sui, J., Biswal, B. B., … Calhoun, V. (2018). Transient increased thalamic-sensory connectivity and decreased whole-brain dynamism in autism. *NeuroImage*. https://doi.org/10.1016/j.neuroimage.2018.06.003

Gow, D. W., Jr. (2012). The cortical organization of lexical knowledge: A dual lexicon model of spoken language processing. *Brain and Language*, *121*, 273–288. https://doi.org/10.1016/j.bandl.2012.03.005

Grady, C. L., McIntosh, A. R., Beig, S., Keightley, M. L., Burian, H., & Black, S. E. (2003). Evidence from functional neuroimaging of a compensatory prefrontal network in Alzheimer's disease. *Journal of Neuroscience*, *23*, 986–993. https://doi.org/10.1523/JNEUROSCI.23-03-00986.2003

Greicius, M. D., Krasnow, B., Reiss, A. L., & Menon, V. (2003). Functional connectivity in the resting brain: A network analysis of the default mode hypothesis. *Proceedings of the National Academy of Sciences of the United States of America*, *100*, 253–258. https://doi.org/10.1073/pnas.0135058100

Greicius, M. D., Srivastava, G., Reiss, A. L., & Menon, V. (2004). Default-mode network activity distinguishes Alzheimer's disease from healthy aging: Evidence from functional MRI. *Proceedings of the National Academy of Sciences of the United States of America*, *101*, 4637–4642. https://doi.org/10.1073/pnas.0308627101

Guo, H., Liu, L., Chen, J., Xu, Y., & Jie, X. (2017). Alzheimer classification using a minimum spanning tree of high-order functional network on fMRI Dataset. *Frontiers in Neuroscience*, *11*, 639. https://doi.org/10.3389/Fnins.2017.00639

Gupta, M., Dasgupta, A., Khwaja, G. A., Chowdhury, D., Patidar, Y., & Batra, A. (2014). Behavioural and psychological symptoms in post-stroke vascular cognitive impairment. *Behavioural Neurology*, *2014*, 430128. https://doi.org/10.1155/2014/430128

Hachinski, V., Iadecola, C., Petersen, R. C., Breteler, M. M., Nyenhuis, D. L., Black, S. E., … Kalaria, R. N. (2006). National Institute of Neurological Disorders and Stroke–Canadian stroke network vascular cognitive

impairment harmonization standards. *Stroke*, *37*, 2220–2241. https://doi.org/10.1161/01.Str.0000237236.88823.47

Hickok, G., & Poeppel, D. (2007). The cortical organization of speech processing. *Nature Reviews Neuroscience*, *8*, 393–402. https://doi.org/10.1038/nrn2113

Hutchison, R. M., & Morton, J. B. (2015). Tracking the brain's functional coupling dynamics over development. *Journal of Neuroscience*, *35*, 6849–6859. https://doi.org/10.1523/JNEUROSCI.4638-14.2015

Hutchison, R. M., Womelsdorf, T., Allen, E. A., Bandettini, P. A., Calhoun, V. D., Corbetta, M., … Gonzalez-Castillo, J. (2013a). Dynamic functional connectivity: Promise, issues, and interpretations. *NeuroImage*, *80*, 360–378. https://doi.org/10.1016/j.neuroimage.2013.05.079

Hutchison, R. M., Womelsdorf, T., Gati, J. S., Everling, S., & Menon, R. S. (2013b). Resting-state networks show dynamic functional connectivity in awake humans and anesthetized macaques. *Human Brain Mapping*, *34*, 2154–2177. https://doi.org/10.1002/hbm.22058

Jack, C. R., Bennett, D. A., Blennow, K., Carrillo, M. C., Dunn, B., Haeberlein, S. B., … Karlawish, J. (2018). NIA-AA research framework: Toward a biological definition of Alzheimer's disease. *Alzheimer's & Dementia*, *14*, 535–562. https://doi.org/10.1016/j.jalz.2018.02.018

Jafri, M. J., Pearlson, G. D., Stevens, M., & Calhoun, V. D. (2008). A method for functional network connectivity among spatially independent resting-state components in schizophrenia. *NeuroImage*, *39*, 1666–1681. https://doi.org/10.1016/j.neuroimage.2007.11.001

Jagust, W. (2001). Untangling vascular dementia. *The Lancet*, *358*, 2097–2098. https://doi.org/10.1016/S0140-6736(01)07230-0

Jantzen, K., Oullier, O., Marshall, M., Steinberg, F., & Kelso, J. (2007). A parametric fMRI investigation of context effects in sensorimotor timing and coordination. *Neuropsychologia*, *45*, 673–684. https://doi.org/10.1016/j.neuropsychologia.2006.07.020

Jin Thong, J. Y., Du, J., Ratnarajah, N., Dong, Y., Soon, H. W., Saini, M., … Qiu, A. (2014). Abnormalities of cortical thickness, subcortical shapes, and white matter integrity in subcortical vascular cognitive impairment. *Human Brain Mapping*, *35*, 2320–2332. https://doi.org/10.1002/hbm.22330

Jones, D., Machulda, M. M., Vemuri, P., McDade, E., Zeng, G., Senjem, M., … Knopman, D. S. (2011). Age-related changes in the default mode network are more advanced in Alzheimer disease. *Neurology*, *77*, 1524–1531. https://doi.org/10.1212/WNL.0b013e318233b33d

Kana, R. K., Keller, T. A., Cherkassky, V. L., Minshew, N. J., & Just, M. A. (2006). Sentence comprehension in autism: Thinking in pictures with decreased functional connectivity. *Brain*, *129*, 2484–2493. https://doi.org/10.1093/brain/awl164

Karas, G., Scheltens, P., Rombouts, S., van Schijndel, R., Klein, M., Jones, B., … Barkhof, F. (2007). Precuneus atrophy in early-onset Alzheimer's disease: A morphometric structural MRI study. *Neuroradiology*, *49*, 967–976. https://doi.org/10.1007/s00234-007-0269-2

Kim, J., Criaud, M., Cho, S. S., Díez-Cirarda, M., Mihaescu, A., Coakeley, S., … Houle, S. (2017). Abnormal intrinsic brain functional network dynamics in Parkinson's disease. *Brain*, *140*, 2955–2967. https://doi.org/10.1093/brain/awx233

Kim, J., Kim, Y.-H., & Lee, J.-H. (2013). Hippocampus–precuneus functional connectivity as an early sign of Alzheimer's disease: A preliminary study using structural and functional magnetic resonance imaging data. *Brain Research*, *1495*, 18–29. https://doi.org/10.1016/j.brainres.2012.12.011

Lehmann, D., Strik, W., Henggeler, B., König, T., & Koukkou, M. (1998). Brain electric microstates and momentary conscious mind states as building blocks of spontaneous thinking: I. Visual imagery and abstract thoughts. *International Journal of Psychophysiology*, *29*, 1–11. https://doi.org/10.1016/S0167-8760(97)00098-6

Li, Y. O., Adalı, T., & Calhoun, V. D. (2007). Estimating the number of independent components for functional magnetic resonance imaging data. *Human Brain Mapping*, *28*, 1251–1266. https://doi.org/10.1002/hbm.20359

Liang, Y., Sun, X., Xu, S., Liu, Y., Huang, R., Jia, J., & Zhang, Z. (2016). Preclinical cerebral network connectivity evidence of deficits in mild white matter lesions. *Frontiers in Aging Neuroscience*, *8*, 27. https://doi.org/10.3389/fnagi.2016.00027

Loewenstein, D. A., Acevedo, A., Small, B. J., Agron, J., Crocco, E., & Duara, R. (2009). Stability of different subtypes of mild cognitive impairment among the elderly over a 2-to 3-year follow-up period. *Dementia and Geriatric Cognitive Disorders*, *27*, 418–423. https://doi.org/10.1159/000211803

Loring, D. W., Meador, K., Mahurin, R. K., & Largen, J. W. (1986). Neuropsychological performance in dementia of the Alzheimer type and multi-infarct dementia. *Archives of Clinical Neuropsychology*, *1*, 335–340. https://doi.org/10.1016/0887-6177(86)90137-X

Lyketsos, C. G., Lopez, O., Jones, B., Fitzpatrick, A. L., Breitner, J., & DeKosky, S. (2002). Prevalence of neuropsychiatric symptoms in dementia and mild cognitive impairment: Results from the cardiovascular health study. *Journal of the American Medical Association*, *288*, 1475–1483. https://doi.org/10.1001/jama.288.12.1475

Marusak, H. A., Calhoun, V. D., Brown, S., Crespo, L. M., Sala-Hamrick, K., Gotlib, I. H., & Thomason, M. E. (2017). Dynamic functional connectivity of neurocognitive networks in children. *Human Brain Mapping*, *38*, 97–108. https://doi.org/10.1002/hbm.23346

Mazzucchi, A., Capitani, E., Poletti, A., Posteraro, L., Bocelli, G., Campari, F., & Parma, M. (1987). Discriminant analysis of WAIS results in different types of dementia and depressed patients. *Functional Neurology*, *2*, 155–163.

McKhann, G., Drachman, D., Folstein, M., Katzman, R., Price, D., & Stadlan, E. M. (1984). Clinical diagnosis of Alzheimer's disease report of the NINCDS-ADRDA work group* under the auspices of Department of Health and Human Services Task Force on Alzheimer's disease. *Neurology*, *34*, 939–939, 944. https://doi.org/10.1212/WNL.34.7.939

Miller, R. L., Yaesoubi, M., & Calhoun, V. D. (2014). *Higher dimensional analysis shows reduced dynamism of time-varying network connectivity in schizophrenia patients.* Engineering in Medicine and Biology Society (EMBC), 2014 36th Annual International Conference of the IEEE. Chicago IL, USA: IEEE, 3837–3840.

Morris, J. C. (1997). Clinical dementia rating: A reliable and valid diagnostic and staging measure for dementia of the Alzheimer type. *International Psychogeriatrics*, *9*, 173–176. https://doi.org/10.1017/S1041610297004870

Ng, H. T., Kao, K.-L. C., Chan, Y., Chew, E., Chuang, K., & Chen, S. A. (2016). Modality specificity in the cerebro-cerebellar neurocircuitry during working memory. *Behavioural Brain Research*, *305*, 164–173. https://doi.org/10.1016/j.bbr.2016.02.027

O'reilly, J. X., Beckmann, C. F., Tomassini, V., Ramnani, N., & Johansen-Berg, H. (2009). Distinct and overlapping functional zones in the cerebellum defined by resting state functional connectivity. *Cerebral Cortex*, *20*, 953–965. https://doi.org/10.1093/cercor/bhp157

Perry, R. J., & Hodges, J. R. (1999). Attention and executive deficits in Alzheimer's disease: A critical review. *Brain*, *122*, 383–404. https://doi.org/10.1093/brain/122.3

Potkins, D., Myint, P., Bannister, C., Tadros, G., Chithramohan, R., Swann, A., … Ballard, C. (2003). Language impairment in dementia: Impact on symptoms and care needs in residential homes. *International Journal of Geriatric Psychiatry*, *18*, 1002–1006. https://doi.org/10.1002/gps.1002

Raichle, M. E., MacLeod, A. M., Snyder, A. Z., Powers, W. J., Gusnard, D. A., & Shulman, G. L. (2001). A default mode of brain function. *Proceedings of the National Academy of Sciences of the United States of America*, *98*, 676–682. https://doi.org/10.1073/pnas.98.2.676

Rashid, B., Arbabshirani, M. R., Damaraju, E., Cetin, M. S., Miller, R., Pearlson, G. D., & Calhoun, V. D. (2016). Classification of schizophrenia and bipolar patients using static and dynamic resting-state fMRI

brain connectivity. *NeuroImage*, *134*, 645–657. https://doi.org/10.1016/j.neuroimage.2016.04.051

Rashid, B., Damaraju, E., Pearlson, G. D., & Calhoun, V. D. (2014). Dynamic connectivity states estimated from resting fMRI identify differences among schizophrenia, bipolar disorder, and healthy control subjects. *Frontiers in Human Neuroscience*, *8*, 897. https://doi.org/10.3389/Fnhum.2014.00897

Román, G. C. (2002a). Vascular dementia may be the most common form of dementia in the elderly. *Journal of the Neurological Sciences*, *203*, 7–10.

Román, G. C., Erkinjuntti, T., Wallin, A., Pantoni, L., & Chui, H. C. (2002b). Subcortical ischaemic vascular dementia. *The Lancet Neurology*, *1*, 426–436.

Rosenberg, G. A. (2017). Binswanger's disease: Biomarkers in the inflammatory form of vascular cognitive impairment and dementia. *Journal of Neurochemistry*, *144*, 634–643. https://doi.org/10.1111/jnc.14218

Rosenberg, G. A., Wallin, A., Wardlaw, J. M., Markus, H. S., Montaner, J., Wolfson, L., … Dichgans, M. (2016). Consensus statement for diagnosis of subcortical small vessel disease. *Journal of Cerebral Blood Flow & Metabolism*, *36*, 6–25. https://doi.org/10.1038/jcbfm.2015.172

Sang, L., Chen, L., Wang, L., Zhang, J., Zhang, Y., Li, P., … Qiu, M. (2018). Progressively disrupted brain functional connectivity network in subcortical ischemic vascular cognitive impairment patients. *Frontiers in Neurology*, *9*, 94. https://doi.org/10.3389/fneur.2018.00094

Sarangi, S., San Pedro, E. C., & Mountz, J. M. (2000). Anterior choroidal artery infarction presenting as a progressive cognitive deficit. *Clinical Nuclear Medicine*, *25*, 187–190. https://doi.org/10.1097/00003072-200003000-00006

Schmahmann, J. D. (2018). The cerebellum and cognition. *Neuroscience Letters*, *688*, 62–75. https://doi.org/10.1016/j.neulet.2018.07.005

Schmahmann, J. D., Weilburg, J. B., & Sherman, J. C. (2007). The neuropsychiatry of the cerebellum—Insights from the clinic. *The Cerebellum*, *6*, 254–267. https://doi.org/10.1080/14734220701490995

Segall, J. M., Allen, E. A., Jung, R. E., Erhardt, E. B., Arja, S. K., Kiehl, K. A., & Calhoun, V. D. (2012). Correspondence between structure and function in the human brain at rest. *Frontiers in Neuroinformatics*, *6*, 10. https://doi.org/10.3389/Fninf.2012.00010

Seo, S. W., Ahn, J., Yoon, U., Im, K., Lee, J. M., Tae Kim, S., … Na, D. L. (2010). Cortical thinning in vascular mild cognitive impairment and vascular dementia of subcortical type. *Journal of Neuroimaging*, *20*, 37–45. https://doi.org/10.1111/j.1552-6569.2008.00293.x

Smith, S. M., Fox, P. T., Miller, K. L., Glahn, D. C., Fox, P. M., Mackay, C. E., … Laird, A. R. (2009). Correspondence of the brain's functional architecture during activation and rest. *Proceedings of the National Academy of Sciences of the United States of America*, *106*, 13040–13045. https://doi.org/10.1073/pnas.0905267106

Sui, J., Pearlson, G., Caprihan, A., Adali, T., Kiehl, K. A., Liu, J., … Calhoun, V. D. (2011). Discriminating schizophrenia and bipolar disorder by fusing fMRI and DTI in a multimodal CCA+ joint ICA model. *NeuroImage*, *57*, 839–855. https://doi.org/10.1016/j.neuroimage.2011.05.055

Sui, J., Pearlson, G. D., Du, Y., Yu, Q., Jones, T. R., Chen, J., … Calhoun, V. D. (2015). In search of multimodal neuroimaging biomarkers of cognitive deficits in schizophrenia. *Biological Psychiatry*, *78*, 794–804. https://doi.org/10.1016/j.biopsych.2015.02.017

Sun, X., Liang, Y., Wang, J., Chen, K., Chen, Y., Zhou, X., … Zhang, Z. (2014). Early frontal structural and functional changes in mild white matter lesions relevant to cognitive decline. *Journal of Alzheimer's Disease*, *40*, 123–134. https://doi.org/10.3233/JAD-131709

Sun, Y.-W., Zhou, Y., Xu, Q., Qian, L.-J., Tao, J., & Xu, J.-R. (2011). Abnormal functional connectivity in patients with vascular cognitive impairment, no dementia: A resting-state functional magnetic resonance imaging study. *Behavioural Brain Research*, *223*, 388–394. https://doi.org/10.1016/j.bbr.2011.05.006

Tucholka, A., Grau-Rivera, O., Falcon, C., Rami, L., Sánchez-Valle, R., Lladó, A., … Initiative, A. S. D. N. (2018). Structural connectivity alterations along the Alzheimer's disease continuum: Reproducibility across two independent samples and correlation with cerebrospinal fluid amyloid-β and tau. *Journal of Alzheimer's Disease*, *61*, 1575–1587. https://doi.org/10.3233/JAD-170553

Wang, K., Jiang, T., Liang, M., Wang, L., Tian, L., Zhang, X., Li, K., & Liu, Z., (2006). *Discriminative analysis of early Alzheimer's disease based on two intrinsically anti-correlated networks with resting-state fMRI.* International Conference on Medical Image Computing and Computer-Assisted Intervention. Berlin: Springer, 340–347.

Wang, K., Liang, M., Wang, L., Tian, L., Zhang, X., Li, K., & Jiang, T. (2007). Altered functional connectivity in early Alzheimer's disease: A resting-state fMRI study. *Human Brain Mapping*, *28*, 967–978. https://doi.org/10.1002/hbm.20324

Yi, L., Wang, J., Jia, L., Zhao, Z., Lu, J., Li, K., … Han, Y. (2012). Structural and functional changes in subcortical vascular mild cognitive impairment: A combined voxel-based morphometry and resting-state fMRI study. *PLoS One*, *7*, e44758. https://doi.org/10.1371/journal.pone.0044758

Yu, Y., Zhou, X., Wang, H., Hu, X., Zhu, X., Xu, L., … Sun, Z. (2015). Small-world brain network and dynamic functional distribution in patients with subcortical vascular cognitive impairment. *PLoS One*, *10*, e0131893. https://doi.org/10.1371/journal.pone.0131893

Zalesky, A., Fornito, A., Cocchi, L., Gollo, L. L., & Breakspear, M. (2014). Time-resolved resting-state brain networks. *Proceedings of the National Academy of Sciences of the United States of America*, *111*, 10341–10346. https://doi.org/10.1073/pnas.1400181111

Zang, Y., Jiang, T., Lu, Y., He, Y., & Tian, L. (2004). Regional homogeneity approach to fMRI data analysis. *NeuroImage*, *22*, 394–400. https://doi.org/10.1016/j.neuroimage.2003.12.030

Zhang, D., Liu, B., Chen, J., Peng, X., Liu, X., Fan, Y., … Huang, R. (2013). Determination of vascular dementia brain in distinct frequency bands with whole brain functional connectivity patterns. *PLoS One*, *8*, e54512. https://doi.org/10.1371/journal.pone.0054512

Zhang, H.-Y., Wang, S.-J., Xing, J., Liu, B., Ma, Z.-L., Yang, M., … Teng, G.-J. (2009). Detection of PCC functional connectivity characteristics in resting-state fMRI in mild Alzheimer's disease. *Behavioural Brain Research*, *197*, 103–108. https://doi.org/10.1016/j.bbr.2008.08.012

Zheng, W., Liu, X., Song, H., Li, K., & Wang, Z. (2017). Altered functional connectivity of cognitive-related cerebellar subregions in Alzheimer's disease. *Frontiers in Aging Neuroscience*, *9*, 143. https://doi.org/10.3389/Fnagi.2017.00143

Zhou, X., Hu, X., Zhang, C., Wang, H., Zhu, X., Xu, L., … Yu, Y. (2016). Aberrant functional connectivity and structural atrophy in subcortical vascular cognitive impairment: Relationship with cognitive impairments. *Frontiers in Aging Neuroscience*, *8*, 14. https://doi.org/10.3389/fnagi.2016.00014

SUPPORTING INFORMATION

Additional supporting information may be found online in the Supporting Information section at the end of this article.

How to cite this article: Fu Z, Caprihan A, Chen J, et al. Altered static and dynamic functional network connectivity in Alzheimer's disease and subcortical ischemic vascular disease: shared and specific brain connectivity abnormalities. *Hum Brain Mapp*. 2019;40:3203–3221. https://doi.org/10.1002/hbm.24591